BBA - Molecular Cell Research 1869 (2022) 119157

Contents lists available at ScienceDirect

BBA - Molecular Cell Research

journal homepage: www.elsevier.com/locate/bbamcr

Mesenchymal stromal cells enhance self-assembly of a HUVEC tubular network through uPA-uPAR/VEGFR2/integrin/NOTCH crosstalk

Irina Beloglazova [a,*], Victoria Stepanova [c,**], Ekaterina Zubkova [a], Konstantin Dergilev [a], Natalia Koptelova [b], Pyotr A. Tyurin-Kuzmin [b], Daniyar Dyikanov [b], Olga Plekhanova [a], Douglas B. Cines [c], Andrew P. Mazar [d], Yelena Parfyonova [a,b]

[a] National Medical Research Center for Cardiology, Moscow, Russian Federation
[b] Department of Biochemistry and Molecular Medicine, Faculty of Medicine, Lomonosov Moscow State University, Moscow, Russian Federation
[c] Department of Pathology and Laboratory Medicine, Perelman School of Medicine, University of Pennsylvania, Philadelphia, PA, USA
[d] Monopar Therapeutics, Wilmette, IL 60091, USA

ARTICLE INFO

Keywords:
Co-culture
Angiogenesis
Urokinase
Integrins
VEGFR2
NOTCH

ABSTRACT

Endothelial cells (ECs) degrade the extracellular matrix of vessel walls and contact surrounding cells to facilitate migration during angiogenesis, leading to formation of an EC-tubular network (ETN). Mesenchymal stromal cells (MSC) support ETN formation when co-cultured with ECs, but the mechanism is incompletely understood. We examined the role of the urokinase-type plasminogen activator (uPA) system, i.e. the serine protease uPA, its inhibitor PAI-1, receptor uPAR/CD87, clearance by the low-density lipoprotein receptor-related protein (LRP1) and their molecular partners, in the formation of ETNs supported by adipose tissue-derived MSC. Co-culture of human umbilical vein ECs (HUVEC) with MSC increased mRNA expression levels of uPAR, MMP14, VEGFR2, TGFβ1, integrin β_3 and Notch pathway components (Notch1 receptor and ligands: Dll1, Dll4, Jag1) in HUVECs and uPA, uPAR, TGFβ1, integrin β_3, Jag1, Notch3 receptor in MSC. Inhibition at several steps in the activation process indicates that uPA, uPAR and LRP1 cross-talk with α_v-integrins, VEGFR2 and Notch receptors/ligands to mediate ETN formation in HUVEC-MSC co-culture. The urokinase system mediates ETN formation through the coordinated action of uPAR, uPA's catalytic activity, its binding to uPAR and its nuclear translocation. These studies identify potential targets to help control aberrant angiogenesis with minimal impact on healthy vasculature.

1. Introduction

Angiogenesis, the development of new vasculature, is a necessary component of many physiological processes during embryonic and postnatal development, including wound healing, ovulation, and placental development [1,2]. Delayed or incomplete angiogenesis leads to tissue ischemia in patients with peripheral artery disease and intermittent claudication, myocardial infarction and ischemic stroke. However, endovascular interventions for these conditions often provide incomplete benefit and may be followed by thrombosis or restenosis. Attempts to stimulate endogenous revascularization have met with limited success and with the concern that excessive angiogenesis is central to the spread of cancer cells, development of diabetic and sickle retinopathy and progression of atherosclerosis itself [3–5], and other pathologies. Therefore, there is a need to better understand the molecular mechanisms and cues involved in angiogenesis, starting with the mechanism by which endothelial cell (EC) growth, migration and tubulogenesis is regulated by the underlying stromal cells, secreted growth factors and cytokines in order to facilitate control the dysfunctional angiogenesis in tumors or vascular related diseases.

New vessel formation is often stimulated by local hypoxia or a gradient of angiogenic agonists, including vascular endothelial growth factor(s) (VEGFs). Sprouting of ECs from existing vessels involves a tightly regulated sequence of events often initiated by binding of VEGF to its receptors (VEGFR1 (Flt-1) and VEGFR2 (KDR)), enhanced adhesion to extracellular matrix proteins, degradation and remodeling of the basement membrane and invasion of adjacent tissue [2,6]. It has been difficult to fully recapitulate these events in vitro. ECs form unstable

* Correspondence to: I. Beloglazova, 3-rd Cherepkovskaya St 15-a, Moscow 121552, Russian Federation.
** Correspondence to: V. Stepanova, 513B Stellar Chance Bld, 422 Curie Blvd, Philadelphia 19104, PA, USA.
E-mail addresses: irina.beloglazova@cardio.ru (I. Beloglazova), vstepano@pennmedicine.upenn.edu (V. Stepanova).

https://doi.org/10.1016/j.bbamcr.2021.119157
Received 2 December 2020; Received in revised form 14 September 2021; Accepted 29 September 2021
Available online 4 October 2021

structures when cultured on Matrigel™ [7]. In contrast, direct contact with vascular mesenchymal cells (MCs) inhibits EC proliferation, stimulates collagen synthesis, and leads to formation of capillary-like endothelial tubular networks (ETNs) [8,9] that are stable for several weeks. A mechanistic understanding of ETN formation may provide insight into the regulation of angiogenesis in vivo.

Angiogenesis and vascular permeability are promoted by urokinase-type plasminogen activator (uPA) through a combination of plasmin-mediated proteolytic degradation of extracellular matrix and intracellular signaling through multiple uPA-binding receptors [10–12]. uPA is secreted as a proteolytically inactive single-chain precursor (scuPA) [13] by ECs and MCs [14]. scuPA binds with high affinity (Kd 0.1–1 nM) to a glycosyl-phosphatidylinositol-(GPI)-anchored receptor (uPAR/CD87, uPAR hereafter). uPAR-bound scuPA can be activated by plasmin via a single peptide bond cleavage, which generates fully enzymatically active two-chain uPA (tcuPA) [15]. Binding to GPI-anchored uPAR, which is mobile in the plasma membrane, permits directional cell migration by localizing bound uPA to the leading edge of migrating cells, where local plasmin-activated matrix metalloproteases (MMPs) degrade matrix and release of matrix bound growth factors [10,16–20]. uPAR also binds to the extracellular matrix protein vitronectin (VN) in a uPA-dependent and -independent manner [21,22], and subsequently with VN-binding receptors $\alpha_v\beta_3$ and $\alpha_v\beta_5$ [23–26] and to the fibronectin-binding integrin $\alpha_v\beta_1$ [23,24]. Together these membrane interactions in cis initiate an intracellular signaling cascade that facilitates cell adhesion and migration. Converting resting ECs into a migrating phenotype involves programmed loss of uPA-dependent adhesion and contemporaneous formation of numerous new short focal contacts [27].

uPAR-bound tcuPA is irreversibly inactivated by the serpin plasminogen activator inhibitor 1 (PAI-1) [28,29]. The resultant tcuPA-PAI-1-uPAR complexes undergo clathrin-dependent endocytosis with the aid of the low density lipoprotein receptor-related protein 1 (LRP1 hereafter) [30]. LRP1-mediated endocytosis leads to lysosomal degradation of the tcuPA-PAI-1 complex [31,32], while uPAR and LRP1 recycle to the cell surface [30]. scuPA also binds LRP1 directly, albeit with lower affinity, and undergoes internalization [31]. Internalization of tcuPA-PAI-1 complexes through LRP1 is accompanied by activation of the intracellular signaling mediators protein kinase A (PKA) [33] and Rac1 [34]. We have shown previously that uPA-PAI-1 complexes regulate endothelial permeability via a LRP1-mediated signaling cascade that involves PKA [35], which may thereby affect angiogenesis as well. uPA also promotes angiogenesis by direct cleavage and activation of VEGF189 [18]. We have also shown that when secreted scuPA exceeds uPAR-binding capacity, the proenzyme translocates to EC nuclei [36] up-regulating VEGFR1 and VEGFR2 expression via transcriptional mechanisms [12].

Mesenchymal cells (MCs) help to drive vessel maturation and regulate vascular function. MCs, like ECs, express uPA, PAI-1, uPAR and LRP1. What is not clear is how mutual coordination of the uPA system between MCs and ECs is established and maintained to permit angiogenesis. In the present manuscript, we examined the role of the uPA system in ETN formation supported by adipose tissue-derived mesenchymal stromal cells (MSC). The results show that α_v-integrins, LRP1, uPAR and VEGFR2 and the components of the Notch pathway orchestrate ETN formation in EC-MSC co-culture. These results provide new insights into the regulation of EC-MC interactions and how they may control physiologic and pathological angiogenesis.

2. Materials and methods

2.1. Cell isolation and culture

MSC were obtained from the human biomaterial collection of the Institute for Regenerative Medicine (Lomonosov Moscow State University, collection ID: MSU_MSC_AD; repository catalogue at www.human.depo.msu.ru). All procedures performed with tissue samples from human donors were in accordance with the Declaration of Helsinki and approved by the Ethic Committee of Lomonosov Moscow State University (IRB00010587), protocol #4 (2018). MSC were isolated from abdominal subcutaneous adipose tissue harvested during surgery from predominantly male patients 21–55 years of age. In each experiment, cells from at least three different donors were used.

MSC were cultured in complete DMEM-GlutaMAX™ (Life Technologies) supplemented with 10% FBS (HyClone) and penicillin/streptomycin (Life Technologies). Human umbilical vein endothelial cells (HUVEC) were isolated according to a published protocol [37] from healthy donors and cultured in complete EGM-2 medium (Lonza). Umbilical cords were collected in the Obstetric Department of the V. I. Kulakov National Medical Research Center for Obstetrics, Gynecology, and Perinatology following written informed consent from all women. All cells were maintained in a humidified chamber incubator at 37 °C and 5% CO_2. MSC and HUVEC were grown until 70% confluent. Cell detachment before co-culture experiments was performed with 0.05% trypsin/EDTA (Gibco). In all experiments, HUVEC were used at passage 3 to 5 and MSC at passage 3 to 7. Flow cytometry analysis confirmed that all HUVEC were CD31 positive (Supplement Fig. 1). In each experiment, cells from at least three different donors were used.

2.2. Direct HUVEC-adipose MSC two-dimensional (2D) co-culture model

HUVEC and MSC were plated individually and were allowed to grow for 24 h. Before harvesting, HUVEC were loaded with 5 μM CellTracker™ Green CMFDA fluorescent dye (Invitrogen) for 40 min according to the manufacturer's protocol or left unstained. To study the time course of ETN formation, MSC were pre-loaded with 2 μM PKH26 Red fluorescent dye (Sigma-Aldrich) per the manufacturer's protocol. MSC and HUVEC were detached, counted and mixed at a ratio of HUVEC:MSC = 1:3. The mixtures of cells were seeded onto 24-well plates at a density of 6×10^4 cells/cm^2 and co-cultured for 2 days in a half volume of complete EGM-2 and half volume of basal EBM-2 + 10% FBS in the presence or absence of inhibitors and/or antagonists. Tubular networks formed by fluorescencenly labeled HUVECs were observed using an Axiovert 200 M inverted microscope and documented using an AxioCam HR digital camera (Carl Zeiss). To quantify ETN formation, the total lengths of the tubular structures were measured in five randomly selected fields on each digital image using ImageJ software, and the results were obtained after each experiment was performed 3 times in triplicate for each condition studied. Statistical analysis was performed as described below (2.11).

2.3. Indirect HUVEC-adipose MSC 2D co-culture model in Transwells

HUVEC were seeded into the wells of 6 or 24-well plate at a density of 6×10^4 cells/cm^2. MSCs, at the same density, added to 0.4 μm Transwells (Falcon) inserts and co-cultured in a half volume of complete EGM-2 and half volume of basal EBM-2 + 10% FBS.

2.4. Inhibitors

Antibodies: 1) to uPAR that blocks uPAR binding to the integrins (ATN-658, 75 μg/ml) [38]; 2) to the growth factor like domain of uPA that prevents binding to uPAR (ATN-292, 100 μg/ml); 3) to the kringle domain of uPA (ATN-291, 180 μg/ml) that prevents nuclear translocation [39]; 4) αv integrin blocking antibodies, 5 μg/ml (SouthernBiotech); 5) mouse control total IgG (Imtek). Recombinant LRP1 receptor-associated protein (RAP) (180 nM) (kind gift of Dr. T. Willnow, MaxDelbrueck Center for Molecular Medicine, Humboldt University, Berlin, Germany) was used as an LRP1 antagonist. The following small molecule inhibitors were used: 1) uPA inhibitor amiloride, 100 μM (Calbiochem), 2) VEGFR2 antagonist DMH4 (TOCRIS bioscience); 3) γ-secretase inhibitor XXI (Compound E), 10 μg/ml (Calbiochem). After 48 h of incubation with antibodies or inhibitors, cells were fixed with 4%

paraformaldehyde in PBS for 15 min. Immunofluorescence was visualized using an Axiovert 200M inverted microscope and documented using an AxioCam HR digital camera (Carl Zeiss). The data were quantified as above (Section 2.2).

2.5. Flow cytometry

Monocultures or a mixture of MSC and HUVEC were plated at a density of 6×10^4 cells/cm^2 and co-cultured for 2 days in half volume of complete EGM-2 and half volume of basal EBM-2 + 10% FBS. The cells were then detached with Accutase (PAA Laboratories GmbH) and stained with antibodies to uPAR (R&D Systems), MMP14 (Abcam), VEGFR1 (Affinity Biosciences), VEGFR2 (Abcam), $\alpha_v\beta_3$ (Sigma-Aldrich/Chemicon), and TGFβ1 (Abcam) followed by DyLight649-conjugated donkey anti-goat antibodies (Jackson) and phycoerythrin (PE)-conjugated anti-CD31 antibodies (BD Biosciences). Isotype-matched immunoglobulins were used as negative controls. Stained cells were analyzed by flow cytometry using MoFlo (Dako Cytomation) for uPAR and FACSCantoTM II (BD Biosciences) for MMP14, VEGFR1, VEGFR2, $\alpha_v\beta_3$, and TGFβ1. For intracellular staining of TGFβ1, cells were fixed with 1% formaldehyde solution and permeabilized with saponin (0.1% in PBS).

2.6. ELISA

Conditioned media from monocultures and MSC-HUVEC co-cultures grown for 48 h in DMEM containing 10% FBS and penicillin/streptomycin were collected, centrifuged at 1000 ×*g*, frozen in liquid nitrogen and stored at −70 °C until assayed. The amounts of uPA, PAI-1, VEGF and TGFβ1 in the conditioned media were measured using Quantikine ELISA kits (DUPA00, DSE100, DB100B and DVE00, respectively, R&D Systems).

2.7. Immunofluorescent staining

Monocultures and MSC-HUVEC co-cultures were grown on glass coverslips in the absence or presence of inhibitors and antagonists. Cells were fixed with 4% formaldehyde, permeabilized with 0.1% Triton X-100 (as indicated) and probed with the following primary antibodies: anti-CD31 (Biolegend), PE-conjugated anti-human CD31 (BD Biosciences), anti-fibronectin Alexa Fluor 488(Abcam) or isotype-matched control immunoglobulins, followed by fluorophore-conjugated secondary Abs: goat anti-rabbit Alexa Fluor 488 (Invitrogen) or goat anti-mouse Alexa Fluor 594 (Invitrogen). Stained cells were visualized using a confocal microscope LSM 780 (Zeiss), Nikon Eclipse Ti microscope or wide field fluorescent Axiovert 200 M Microscope (Zeiss).

2.8. RNA isolation, reverse transcription and real-time quantitative PCR

HUVEC and MSC were detached with trypsin/EDTA from monocultures, counted and mixed as above. Cell mixtures were plated at a density of 6×10^4 cells/cm^2 and co-cultured for 24 h in DMEM + 10% FBS + penicillin/streptomycin. MSC and HUVEC or co-cultures were detached with trypsin/EDTA and washed free of trypsin. Cells from co-cultures were separated using flow cell sorter MoFlo (Dako Cytomation). Supplement Fig. 2(C-F) shows the efficacy of cell separation. Total RNA was isolated from MSCs or HUVEC either grown in monoculture or separated from co-culture using RNeasy Mini Kit (QIAGEN). First strand cDNA was synthesized with oligo(dT)-primer using RevertAidTM First Strand cDNA Synthesis Kit (Fermentas). PCR was performed with SYBR Green intercalating dye (Syntol) using a StepOnePlusTM Real-Time PCR System (Applied Biosystems); primers used for PCR are listed in Supplement Table 1. Reaction mixtures (25 μl) contained 1–5 ng of cDNA, 10 pmol of each primer, 10 μl of dNTP/DNA polymerase solution (Sintol) and deionized water up to 25 μl. Control mixtures contained all components except the cDNA template was replaced by deionized water. After denaturation (95 °C, 10 min), 40 amplification cycles were performed for all primer pairs with annealing/elongation at 60 °C for 60 s. Specificity of amplification was analyzed by melting stage upon PCR completion.

2.9. Translocation of uPA to cell nuclei

Iodination of scuPA was performed using Na^{125}I (PerkinElmer) and Iodogen-coated tubes (Pierce/Thermo Scientific) as described [36]. ^{125}I-scuPA (10 nM) was added to HUVEC in 6-well plates for 60 min at 37 °C in triplicates in the absence or presence of mouse monoclonal ATN-291 antibody which recognizes the kringle domain of uPA, ATN-292 antibody which recognizes the GFD of scuPA [39], or isotype control antibody as the negative control. The cells were washed 3 times with PBS. Glycine-HCl buffer (100 mM; pH 3.0) supplemented with 100 mM NaCl was added for 5 min to remove surface-associated ligand and collected. The cells were detached from the culture vessel surface with 0.05% trypsin/EDTA (Gibco), collected and pelleted at 500 g for 5 min at 4 °C. To isolate nuclei, cells were fractionated as described [36]. All manipulations were performed on ice and centrifugations were performed at 4 °C. Briefly, the cells were homogenized in lysis buffer A (20 mM HEPES, pH 7.0, 10 mM KCl, 2 mM $MgCl_2$, 0.5% NP-40), and protease inhibitor cocktail (Sigma-Aldrich) with 30 strokes in a Dounce homogenizer. Homogenates were centrifuged at 1500*g* for 5 min. The nuclear pellets were washed twice. Separated subcellular fractions were counted in a γ-counter to quantify incorporated radioactive protein. Absolute amounts of cell-associated proteins in each fraction were normalized per 10^6 cells.

2.10. Cell treatments, lysis and immunoblotting analysis

MSC and HUVEC were grown in culture dishes for 48 h in monocultures or in co-culture at a density 6×10^4 cells/cm^2 as described above in the absence or presence of the anti-uPA antibody (ATN291), isotype control IgG, inhibitor of γ-secretase XXI (Compound E) (see above), or recombinant soluble Jag1 ligand (sJAG1-Fc; 50 μg/ml; R&D Systems). The cells were then detached with trypsin/EDTA solution and HUVEC were separated from MSCs using the Dynabead® magnetic beads (Thermo Scientific) coated with mouse anti-human ICAM-2 Abs (BioLegend). Supplement Fig. 2(A, B) shows the efficacy of cells separation. Separated cells and the cells from monocultures detached the same way were pelleted by centrifugation and lysed in RIPA buffer (Cell Signaling Technology) supplemented with the 1× proteinase inhibitor cocktail for mammalian culture (Sigma). Protein concentrations in cell lysates were measured using the Bradford Protein Assay (Bio-Rad). Lysates were subjected to SDS-PAGE and Western Blotting using the following primary antibodies: mouse anti-uPA monoclonal antibodies (Imtek, Moscow) which recognize both free uPA and uPA/PAI-1 complexes, rabbit anti-VEGFR2 Abs (Abcam), and rabbit anti-β-actin Abs (Cell Signaling Technology). Secondary HRP-conjugated goat anti-mouse and anti-rabbit Abs (Jackson) were used for detection. HRP-labeled protein bands were visualized using the SuperSignal™ West Femto Maximum Sensitivity Substrate (Thermo Fisher Scientific). Luminescent signals on the blots were scanned and quantified using a Li-COR C-Digit Blot scanner (LI-COR Biosciences)/Image Studio™ software (LI-COR Biosciences). Each experiment was performed in triplicate. Statistical analysis was performed as described below (Section 2.11).

2.11. Statistical analysis

Data are expressed as mean ± standard deviation (SD). Statistical significance of difference between values (unless indicated) was determined using Mann-Whitney for two groups and Kruskal-Wallis for three or more groups followed by Dunn's test for multiple comparisons. $P < 0.05$ was considered significant.

For western blot data analysis we used Student's *t*-tests for single comparisons and analysis of variance (ANOVA) with Dunnett's multiple

comparisons test (data passed Shapiro-Wilk normality test, $P < 0.05$, was considered significant). Data from a minimum of three independent experiments are presented unless stated otherwise.

3. Results

3.1. Kinetics and requirements for ETN formation

Experiments were performed to delineate how coordination between the uPA system in EC and MSC facilitates angiogenesis. We used a 2D direct co-culture model to induce endothelial tubular network (ETN) formation by HUVEC in presence of the adipose stromal tissue-derived mesenchymal cells (MSC) to simulate their proximity in the vessel wall during capillary formation and sprouting [8]. When MSC were plated with HUVEC at a HUVEC:MSC ratio of 1:3, ETN formed in the absence of exogenously added matrix proteins (Fig. 1) while other ratios 3:1 or 1:1 did not generate completed tubular structures (Supplement Fig. 3). Formation of tubular structures was never observed in monocultures of HUVEC (Fig. 1B, Supplement Fig. 4) or MSC (Fig. 1C).

ETN formation became evident by 14 h in co-culture with a sharp increase in total tube length by 25 and 41 h, as visualized using time-lapse video microscopy (Fig. 2A, B, and Movie 1; Supplement Data) and was extensive by 48 h (Fig. 1; panel "co-culture").

The timing of ETN formation tracked with the timing of fibronectin expression and assembly by MSC. Extensive branching of ETN structures was observed when fibronectin fibrils were clearly visible by immunofluorescence 48 h after the MSC and HUVEC were brought into direct co-culture (Fig. 3, Table 1).

However, if MSC were first grown as a monoculture for 48 h to allow fibronectin synthesis, secretion and fibril assembly, and HUVEC were then plated on the top of "48 h-old" MSC, extensive ETN formation by HUVEC was readily evident within 24 h (Fig. 4D-F, and Table 2), whereas after 24 h of direct HUVEC-MSC co-culture both fibronectin fibrils assembly and ETN formation were significantly lower (Fig. 4A-C) and Table 2, row: "Time of MSC monoculture prior co-culture - 0 h".

3.2. Cell-to-cell contacts are required for ETN formation by HUVEC in co-culture with MSC

We next asked whether direct cell-to-cell contact between the HUVEC and MSC is essential to form ETNs. To address this question, we used a Transwell system to study indirect co-culture. HUVEC were plated in the wells of 24-well plates. MSC were plated within the Transwell inserts and placed into the wells of 24-well plates containing the growing HUVEC (Supplement Fig. 5). HUVECs did not form ETN in the absence of direct contact with MSC (Supplement Fig. 4 (Transwell Panels)). In the migration assay MSC plated in 24-well plate ("receiver plate") secreted the factors that stimulated migration of HUVEC (Supplement Fig. 5A) through the 8 μm membrane pores of Transwell inserts (Supplement Fig. 5B and C).

3.3. Involvement of uPA, uPAR and LRP1 in ETN formation

We previously reported that ETN formation on Matrigel requires uPA [12], PAI-1 and uPAR [40]. Based on these observations, we used real-time RT-PCR to study how the co-culture conditions affected the expression of these components of the uPA system, a subset of integrins and pro-angiogenic growth factors, including VEGF and TGFβ1 and receptors implicated in cell adhesion and migration. MSC and HUVEC were grown either as monocultures or were cultured in direct or indirect co-culture for 24 h, the cells were detached from the culture vessel and separated by FACS. mRNA levels were measured by qRT-PCR. Direct co-culture significantly increased uPAR, MMP14, VEGFR2, integrin β3, and TGFβ1 mRNA levels in HUVEC (Fig. 5A), and uPA, uPAR, integrin β3 and

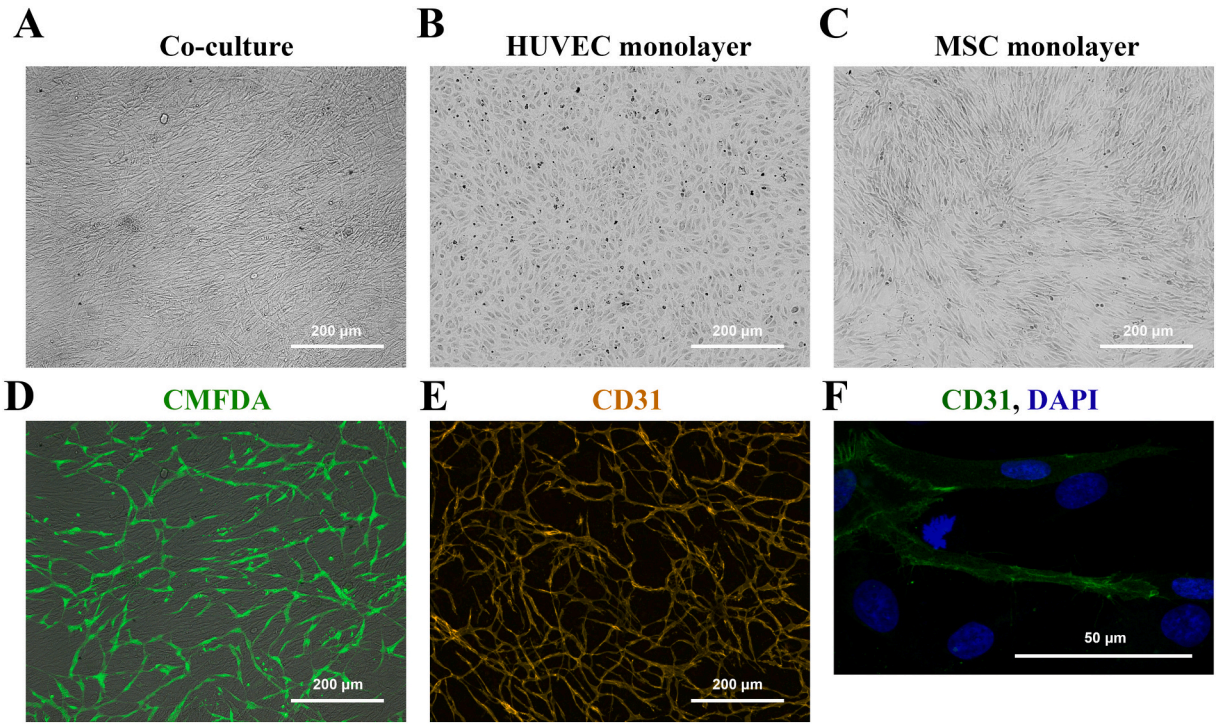

Fig. 1. Induction of ETN formation by HUVEC in direct 2D co-culture with MSC. (A) MSC and HUVEC were co-cultured at a density of 60,000 cells/cm^2 in 24 well plates (120,000 cells total per well) at a HUVEC:MSC ratio of 1:3. Representative images of HUVEC (B) and MSC (C) cultured as monocultures. To visualize the tubular network, HUVEC were either pre-loaded with CMFDA (green) before initiation of co-culture (D) or fixed after 48 h post-initiation of co-culture and stained for CD31 using PE-conjugated anti-CD31 antibody (E), or anti-human CD31 mouse monoclonal antibodies followed by Alexa 488-conjugated anti-mouse antibodies (F). DAPI was used to visualize the nuclei. Images were taken using the Axiovert 200 M Microscope (Zeiss) (A, B, C, D, E panels) and LSM 780 (Zeiss) Microscope (Panel F).

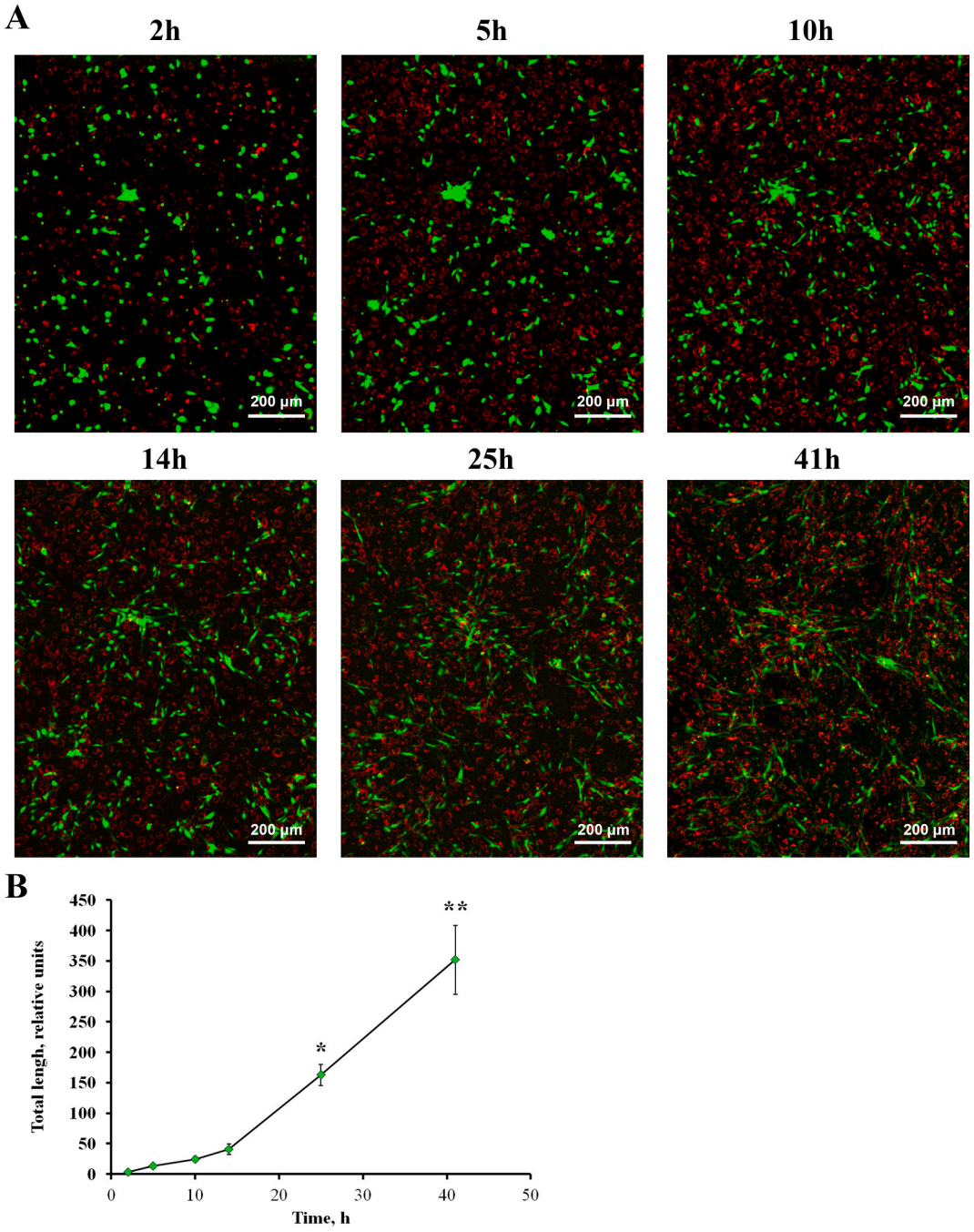

Fig. 2. Time course of induction of ETN formation by MSC. (A) HUVEC were preloaded with CMFDA (green) and MSC with PKH26 (red) before placing them in co-culture. Co-cultures were initiated as in Fig. 1. The cultures were visualized at indicated times after start of co-culture. Time-lapse imaging was performed using an inverted widefield fluorescent microscope Nikon Eclipse Ti Auto Imaging System equipped with an objective CFI Plan Fluor DLL 10X/0.3 (Nikon, Tokyo, Japan) and with digital cooled monochrome CCD camera Nikon DS-Qi1 (Nikon, Tokyo, Japan). Simultaneous acquisition of 6 × 6 fields in Large Image mode was performed within one well of the multi-well culture plate and the images were automatically stitched by the NIS-Elements (Nikon). (B) Quantification of the total lengths of the tubular structures formed by HUVEC co-cultured with MSC at 2, 5, 10, 14, 25 and 41 h performed using Image J software. Data are presented as mean ± SD of total lengths of the tubes per scanned area (number of wells = 3), expressed in relative units. Scale Bar = 200 μm. "*" $P < 0.05$, "**" $P < 0.005$.

TGFβ1 mRNA levels in MSC (Fig. 5B). This indicates that direct contact between the HUVEC and MSC during 24 h changed expression profiles in both cell types. These changes in mRNA levels were accompanied by a greater than 2-fold increase in cell surface-associated uPAR in HUVEC (Fig. 5G) and 2-fold increase of uPA secreted into the media by co-cultured HUVEC and MSC compared to HUVEC in monoculture (Fig. 5D). In contrast, direct HUVEC-MSC co-culture did not change the amounts of secreted PAI-1 compared with HUVEC and MSC in monoculture (Fig. 5C). Fig. 5E shows that MSC secreted much higher levels of VEGF in monoculture (9.5 ± 3 pg/1000 cells) than HUVEC (0.03 ± 0.014 pg/1000 cells). However, VEGF levels in conditioned medium decreased when HUVEC were co-cultured with MSC compared to MSC in monoculture. This suggests that VEGF secreted by MSC was bound and utilized by the HUVEC in co-culture. The increase of MMP14 and VEGFR2 in HUVEC (Fig. 5H and K) and integrin $\alpha_v\beta_3$ in MSC (Fig. 5I) was confirmed by flow cytometry.

In that we observed significant up-regulation of uPA mRNA in MSC during co-culture with HUVEC (Fig. 5B), we asked how uPA system may

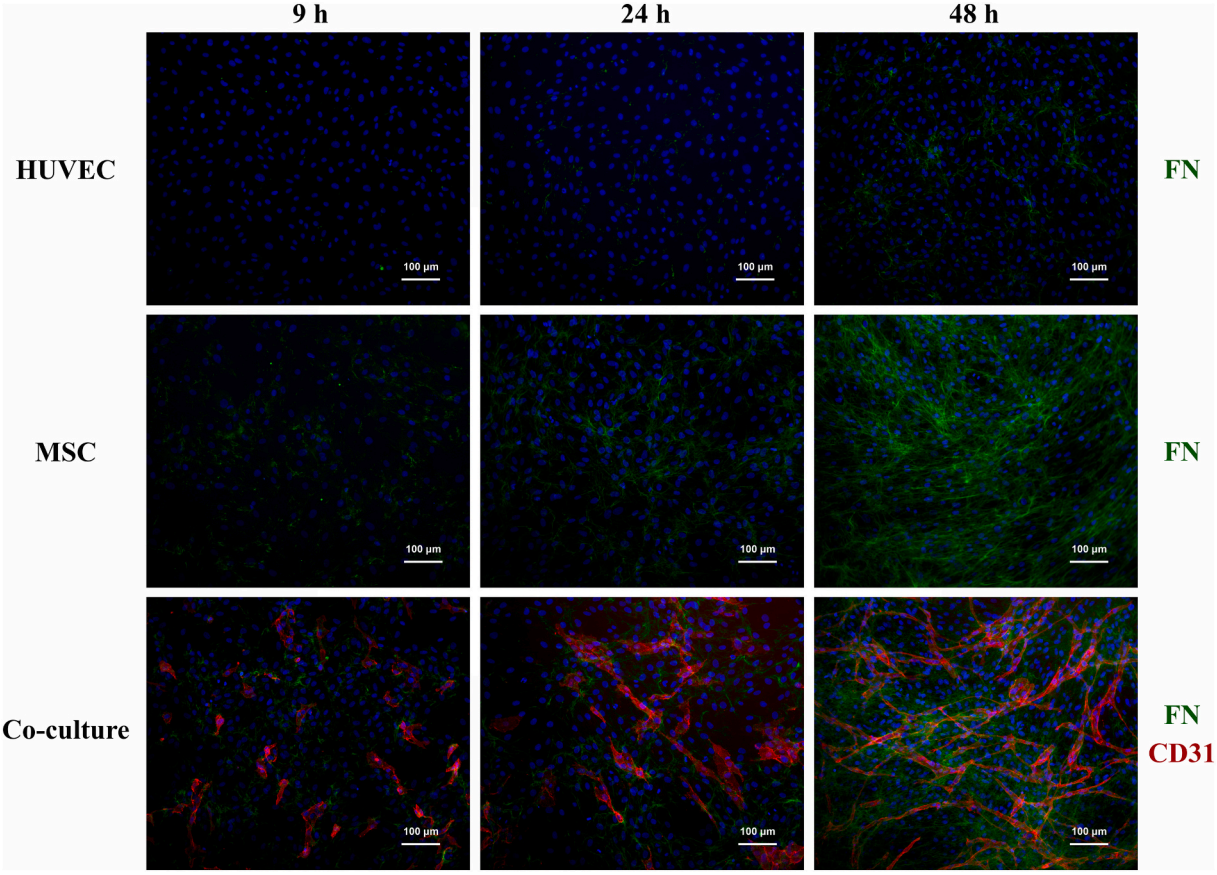

Fig. 3. Dynamics of fibronectin expression by HUVECs and MSCs grown in monocultures (top and middle panels, respectively) and fibronectin expression + tubulogenesis of HUVEC grown in co-culture with MSC (bottom panels). HUVEC, MSC were grown as monoculture or in direct co-culture for 9, 24 and 48 h. Both cell types, cultured for indicated times as monocultures or in direct co-culture, were washed, fixed with 4% PFA, and stained with rabbit anti-fibronectin antibody conjugated with Alexa Fluor 488 (green). The nuclei were counterstained with DAPI (blue). Cells in direct co-cultures were also stained using the anti-CD31 mouse monoclonal antibody followed by Alexa 594-conjugated anti-mouse antibody (red) to depict tubular structures formed by HUVECs. Images were taken using Nikon Eclipse Ti microscope. Scale Bar = 100 μm. Quantification of the intensities of staining for FN, and the total lengths of the tubular structures formed by HUVEC co-cultured with MSC at 9, 24, and 48 h was performed for the "co-culture" panels using Image J software, and results are shown in Table 1. 7 microscopic fields were analyzed per each experimental condition.

Table 1
Quantification of the images prepared for Fig. 3 (co-culture panels) showing the intensities of staining for FN and the total lengths of the tubular structures formed by HUVEC co-cultured with MSC at time points 9, 24, and 48 h.

Co-culture time	FN intensity, a.u./fold increase over 9 h time point	Total length of the tubes, a.u./fold increase over 9 h time point
9 h	1.5 ± 0.4/1 ± 0.3	1.2 ± 0.8/1 ± 0.6
24 h	3.3 ± 0.4/2.2 ± 0.3*	5.6 ± 2.8/4.7 ± 2.4*
48 h	6.7 ± 1.4/4.6 ± 1.0**	31.5 ± 7.7/26.4 ± 6.5**

* $P < 0.05$.
** $P < 0.005$.

contribute to ETN formation by HUVEC in co-culture with MSC in our settings. We used specific reagents to block either uPA or uPAR or to prevent uPA-uPAR association. Fig. 6A and Supplement Fig. 6 shows that the monoclonal antibody ATN-292, which recognizes the growth factor-like domain of uPA (GFD) and therefore blocks uPA binding to uPAR [39], and a function-blocking anti-uPAR antibody (ATN-658) inhibited ETN formation by 32 ± 9% and 32 ± 12%, respectively ($p <$ 0.005 vs mIgG1k). These data suggest that (1) binding of uPA to uPAR contributes to ETN formation by HUVEC induced by MSC; and (2) other uPA (and non-uPA) processes are implicated in ETN formation by HUVEC co-cultured with MSC.

uPA may contribute to ETN formation through its proteolytic activity or via intracellular signaling pathways initiated through uPAR, LRP1 or other endocytic mechanisms. The inhibitor of uPA protease activity amiloride inhibited ETN formation by 66 ± 16% ($P < 0.005$ vs control) (Fig. 6B). This suggests involvement of uPA protease -dependent processes in addition to its binding to uPAR. The uPA protein inhibitor PAI-1, which is expressed by both types of cells (Fig. 5C), irreversibly binds enzymatically active tcuPA and forms catalytically inactive uPA/PAI-1 complexes [41,42]. uPAR-bound tcuPA-PAI-1 complexes undergo endocytosis and degradation via LRP1 [30]. Therefore, we next considered the involvement of the endocytosis of uPA/PAI-1 complexes via LRP1. The LRP1 antagonist receptor associated protein (RAP) [43] inhibited ETN formation by 59.6 ± 20% (P < 0.005 vs control) (Fig. 6B, and Supplement Fig. 6). Together, these data suggest that both the proteolytic activity of uPA and intracellular signaling initiated by binding of uPA to uPAR and internalization of PAI-1-uPA-uPAR complexes via LRP1 contribute to ETN formation. However, as we observed incomplete inhibition of ETN formation in HUVEC-MSC co-culture by RAP and amiloride, we asked whether other uPAR and LRP1 partners are involved in ETN formation during HUVEC-MSC co-culture. We investigated whether α_v-associated integrins ($\alpha_v\beta_3$, $\alpha_v\beta_5$ or $\alpha_v\beta_1$) are involved in ETN formation in HUVEC in co-culture with MSCs. Fig. 6A and Supplement Fig. 6 shows that the α_v neutralizing antibody (anti-CD51) totally abrogated ETN formation in HUVEC-MSC co-culture.

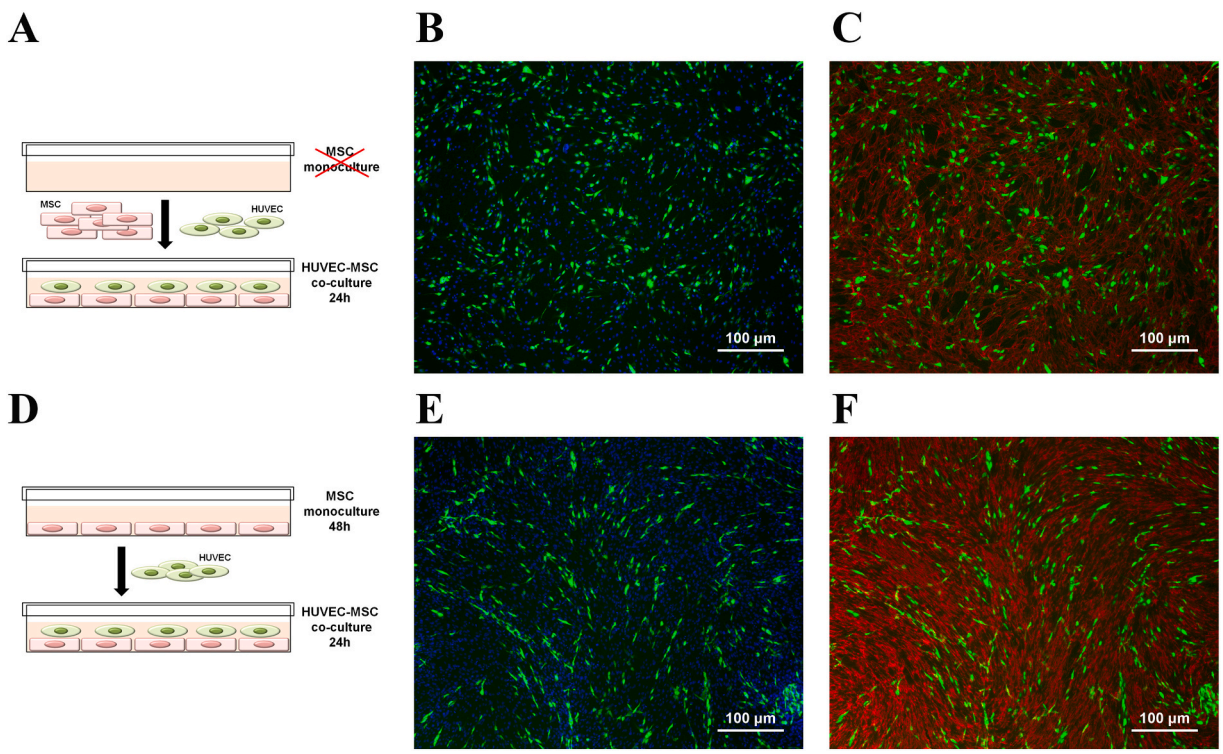

Fig. 4. FN synthesis by MSC accelerates ETN formation by HUVECs in direct co-culture. Panels A and D show schematic re-presentations of various experimental conditions. (A-C) MSCs were mixed with HUVEC, preloaded with CMFDA (green), and co-cultured for 24 h. (D-F) MSC were grown as a monoculture for 48 h ("48 h-old MSCs") to allow synthesis/secretion/assembly of FN fibrils. HUVECs preloaded with CMFDA (green) were then seeded on the top of "48 h-old MSCs" and co-cultured for additional 24 h. Cells were fixed as in Fig. 3, stained with rabbit anti-fibronectin antibody, followed by Alexa594-conjugated anti-rabbit antibody (red). The nuclei were counterstained with DAPI (blue). Images were taken using the Axiovert 200 M Microscope (Zeiss). Representative images of ETN (green) formed by HUVECs after 24 h direct co-culture with MSC, or HUVEC seeded on the top of "48 h-old MSCs" are shown in panels "B" and "E", respectively. Panels "C" and "F" represent merges of the green and red channels to show ETN (green) and fluorescently stained FN (red) for conditions A and D, respectively. Scale Bar = 100 μm. Quantification of the intensities of FN staining per microscopic field and the total lengths of the tubular structures formed by HUVEC co-cultured with MSC in various settings (A and D) were studied as in Fig. 3, and results are shown in Table 2. 7 microscopic fields were analyzed per each experimental condition.

Table 2
Quantification of the images used for Fig. 4, showing the intensities of staining for FN, and the total lengths of the tubular structures formed by HUVEC directly co-cultured for 24 h with MSC (0 h), and seeded on the top of "48 h-old MSCs" (48 h, respectively).

Time of MSC monoculture prior co-culture	FN, a.u./fold increase vs "0 h"	Total lengths of the tubes, a. u./fold increase vs "0 h"
0 h	20.6 ± 1.9/1.0 ± 0.1	2.4 ± 0.6/1.0 ± 0.3
48 h	34.8 ± 4.9/1.7 ± 0.2**	14.5 ± 5.9/6.0 ± 2.5**

** $P < 0.005$.

3.4. Involvement of uPAR partners VEGF/VEGFRs in ETN formation

Binding of VEGF to VEGFR2 stimulates ETN formation [44]. Since we observed up-regulation of VEGFR2 mRNA (Fig. 5A) in HUVEC upon co-culture with MSC, we asked whether blocking VEGFR2 attenuates ETN formation. The VEGFR2 antagonist DMH4 inhibited ETN formation in co-culture in a concentration-dependent manner (Fig. 6C, Supplement Fig. 7).

We then investigated the mechanism through which VEGFR2 expression is upregulated in HUVECs upon co-culture with MSC. We previously reported that scuPA translocates to the nuclei of lung microvascular ECs where it up-regulates VEGFR2 expression via transcriptional mechanisms [12]. Therefore, we asked whether uPA, which is induced in MSC in co-culture, translocates to the nuclei of HUVEC and thereby up-regulates VEGFR2 expression. Translocation of scuPA to cell nuclei depends on its kringle domain [36]. We examined if the monoclonal antibody ATN-291, which binds the kringle domain of human uPA [39], (i) inhibits ETN formation in co-culture with MSC; and (ii) prevents nuclear translocation of scuPA. Our data indicate that ATN291 inhibits ETN formation by HUVECS in co-culture with MSC by 24.5 ± 9.9% (Fig. 7A). The data in Fig. 7B shows that ATN-291 inhibits both surface binding and nuclear translocation of exogenously added recombinant ^{125}I-scuPA in HUVECs, whereas the monoclonal antibody ATN-292, which recognizes the GFD of uPA and blocks its binding to uPAR [39], inhibits surface binding but only slightly inhibits nuclear translocation.

Based on the observation that ATN-291 inhibited ETN formation (Fig. 7A, Supplement Fig. 6), we asked if this antibody also attenuates up-regulation of VEGFR2 in HUVEC co-cultured with MSC. Fig. 7C and D show that up-regulation of VEGFR2 protein in HUVECs upon co-culture with MSCs is inhibited by ATN-291, suggesting that MSC-derived uPA contributes to the mechanism of up-regulation of VEGFR2 expression in HUVEC via a transcriptional mechanism (Fig. 7E) as we described previously [12].

3.5. Involvement of Notch signaling in uPA system-mediated ETN formation in co-culture with MSC

In that we observed robust up-regulation of uPA mRNA in MSC during co-culture with HUVEC (Fig. 5B), and we have shown that the uPA system may contribute to ETN formation by HUVEC in co-culture with MSC via several proteolysis-dependent and -independent pathways (Figs. 6 and 7), we next asked what mechanisms mediate up-regulation of uPA expression in MSC upon uPA-MSC direct co-culture

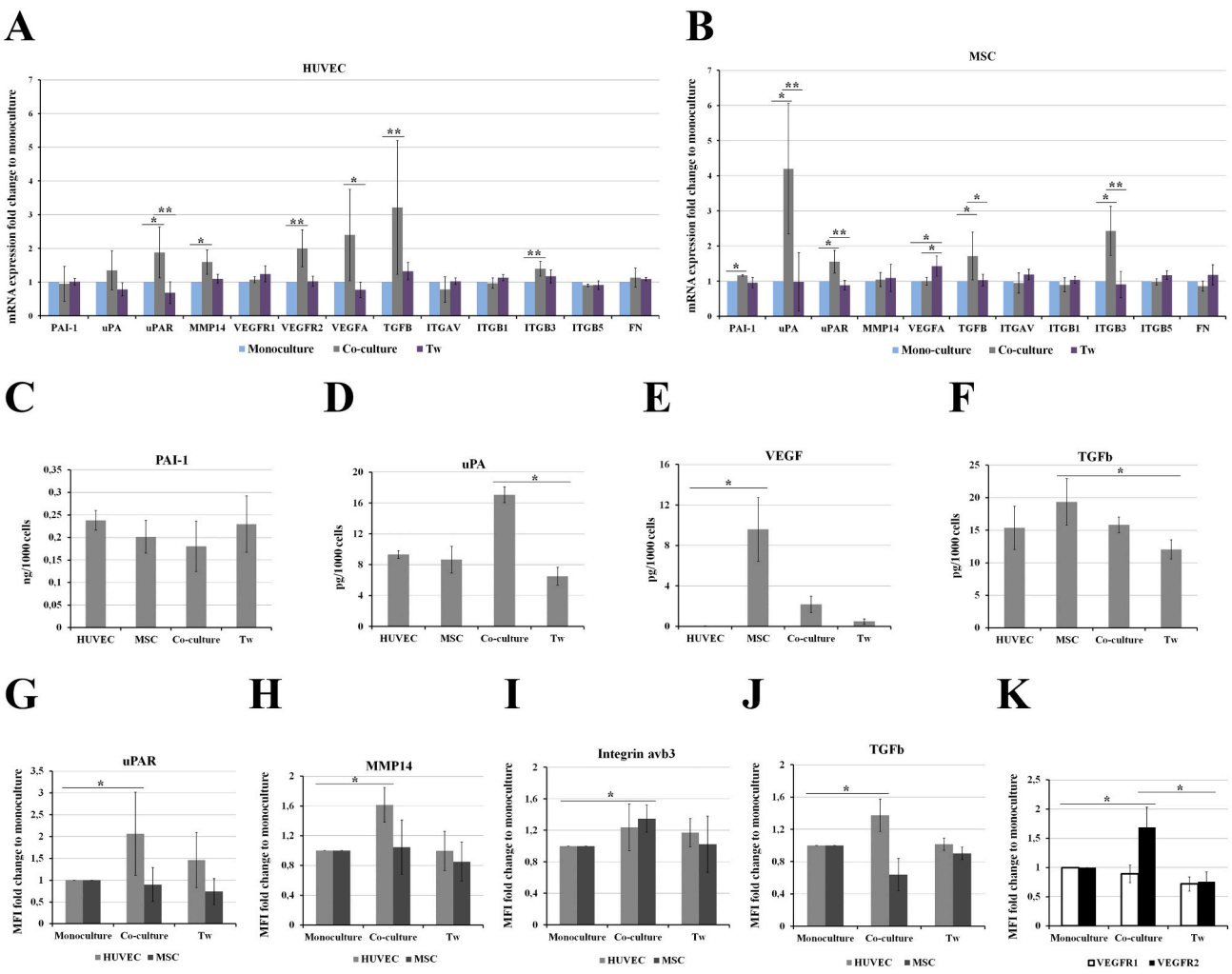

Fig. 5. Direct co-culture of HUVEC and MSC changes the expression profiles in both cell types. HUVEC were preloaded with CMFDA before being placed in direct co-culture (co-culture), monoculture or in indirect co-culture using the semi-permeable Transwell (Tw). MSC and HUVEC were grown as monoculture or co-cultured for 24 h. Cells in direct co-culture were separated using flow cytometry cell sorter. Total RNA was isolated and specific mRNA levels were quantified by qRT PCR as described in "Methods". (A, B) Quantification of changes of mRNA levels in HUVEC (A) and MSC (B) grown in co-culture (grey bars) or Tw (violet bars) vs corresponding monoculture (blue bars) taken as a reference. Y-axis denotes fold changes of mRNA levels of cells in co-culture or Tw compared to the mRNA levels for the same transcript in either HUVEC or MSC monocultures. "*": $P < 0.05$, "**": $P < 0.005$ vs monoculture. $n \geq 3$ experiments. (C-F) MSC and HUVEC were placed in monoculture, indirect (Tw) or direct co-culture for 48 h. Protein levels for PAI-1 (C), uPA (D), VEGF (E) and TGFβ (F) in conditioned media were assessed by ELISA. Y-axis shows absolute amounts of the indicated proteins as pg/1000 cells. "*": $P < 0.05$. (G-K) Relative quantitation of uPAR (G), MMP1 4 (H), integrin $\alpha_v\beta_3$ (I) or TGFβ (J) in HUVECs (light grey bars) and MSC (dark grey bars), and (K) VEGFR1 (white bars) and VEGFR2 (black bars) in HUVECs grown as monocultures, indirect (Tw) or direct co-culture for 48 h. Protein levels were assessed by flow cytometry, as described in "Methods". Y-axis denotes fold change in mean fluorescence intensity (MFI) on either cell type grown in co-culture or Tw vs monoculture. "*": $P < 0.05$ vs monoculture. $n \geq 3$.

and how this contributes to ETN formation by HUVEC in co-culture with MSC.

It was previously reported that uPA is a transcriptional target of the JAG1-Notch receptor signaling in breast cancer cells [45]. Notch signaling pathway is a molecular mechanism that helps coordinate the cellular events that occur during ETN formation in co-culture [46,47]. Therefore, we first asked whether the Notch pathway is activated in MSC and/or HUVEC during their direct co-culture in our settings. We found that direct co-culture of HUVEC with MSCs increased: (i) Jagged 1 (JAG1) ligand 10.16 ± 2 fold ($p < 0.05$ vs monoculture) in MSC and 1.99 ± 0.82 fold, ($p < 0.05$ vs monoculture) in HUVEC; (ii) Notch1 receptor expression (1.77 ± 0.60 fold and 2.56 ± 0.44 fold $p < 0.005$ vs monoculture) in HUVEC and MSC, respectively; (iii) Notch3 receptor expression (3.87 ± 1.07 fold ($p < 0.005$ vs monoculture)) in MSC (Fig. 8B), indicating that HUVEC-MSC co-culture caused a robust induction of Notch signaling in both cell types.

The Notch pathway is known to be abrogated by γ-secretase inhibition [48]. Therefore, we next asked whether inhibition of the Notch pathway would affect ETN formation during HUVEC-MSC co-culture. Fig. 8C shows that Compound E, an inhibitor of γ-secretase (which prevents NCID generation and its nuclear translocation [48]), inhibits ETN formation by 45.7 ± 13% ($p < 0.005$) (See also representative images of ETN formed by HUVECs in co-culture with MSC without or in presence of γ-secretase inhibitor, Supplement Fig. 6 "γ-secretase inhibitor" panel vs "DMSO" panel).

These results led us to ask if the Notch pathway links ETN formation by HUVEC and induction of uPA expression in MSC during their direct co-culture with HUVEC. Our data indicate that Compound E prevented up-regulation of uPA mRNA in MSC in co-culture with HUVECs compared to MSC grown as monocultures (Fig. 8D). Compound E and recombinant soluble Fc-JAG1 protein disrupted up-regulation of uPA protein in MSC co-cultured with HUVEC (Fig. 8E, F).

Our data indicate that (i) VEGFR2 is significantly up-regulated in HUVEC upon co-culture with MSC (Fig. 5A); (ii) uPA is dramatically up-

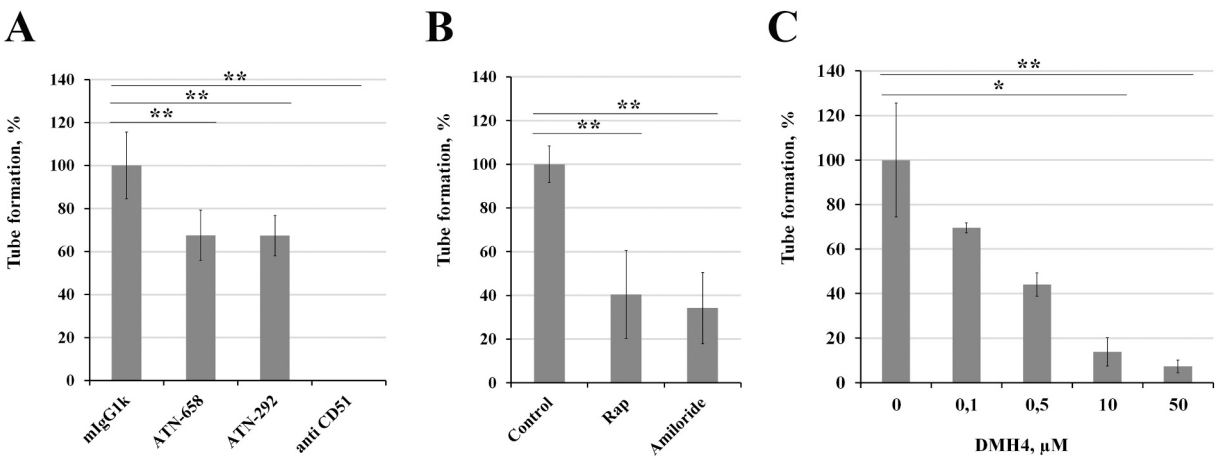

Fig. 6. Effect of inhibitors, blocking antibodies and receptor antagonists on ETN formation by HUVEC co-cultured with MSC. Quantification of the changes in total length of the tubular structures formed by HUVEC co-cultured with MSC for 48 h (as in Fig. 3) in the absence or presence of: (A) anti-uPAR antibodyATN-658 (75 μg/ml), anti-uPA antibody ATN-292 (100 μg/ml), anti-α_v (CD51) blocking antibody (5 μg/ml), mouse IgGk (5, 75, 100 μg/ml); (B) LRP1 antagonist RAP (180 nM), the uPA inhibitor Amiloride (100 μM). (C) VEGFR2 antagonist DMH4 (0.1–50 μM). Y-axis denotes % inhibition. "*"P < 0.05, "**"P < 0.005, n ≥ 3 experiments.

regulated in MSC upon co-culture with HUVEC (Fig. 5B); (iii) Notch pathway mediates both up-regulation of uPA in MSC upon co-culture with HUVEC (Fig. 8D); and ETN formation by HUVEC in co-culture with MSC (Fig. 8C); and (iv) uPA up-regulates expression of VEGFR2 in endothelial cells [12]. Therefore, we asked if Notch pathway inhibitors, which disrupt uPA induction in MSC during co-culture with HUVEC (Fig. 8E, and F), would also prevent VEGFR2 up-regulation in HUVEC co-cultured with MSC. Fig. 8G, and H indeed demonstrate that Compound E and recombinant Fc-JAG1 prevent VEGFR2 up-regulation in HUVEC upon co-culture with MSC. These data further suggest involvement of Notch signaling in regulating uPA-dependent ETN formation by HUVEC in co-culture with MSC (Fig. 8I).

4. Discussion

Modulation of exuberant angiogenesis is a promising approach to help to control cancer [49,50], macular degeneration, diabetic and sickle cell retinopathy [51], rheumatoid arthritis [52], and diverse other disorders. Pathologic angiogenesis involves perturbations in the heterotypic interactions between ECs and stromal cells that maintain vascular integrity, replacement of senescent vessel wall cells and physiologic wound healing. The focus of the current study was to examine in detail the involvement of the uPA system in endothelial cell tube formation, a model of cell-cell and cell-matrix contacts that simulate early steps in the angiogenic process [10].

Co-culture of HUVEC with MSC for 24 h upregulated uPA mRNA in HUVEC (Fig. 5A) and even more strongly in MSC (Fig. 5B) along with an increase in uPA secreted into the media compared with either cell type in monoculture (Fig. 5D). Co-culture also increased uPAR mRNA and protein expression in HUVEC (Fig. 5A, G). There are several mechanisms that may contribute to the upregulation of uPA and uPAR in co-culture of HUVEC with MSC, including stimulation by VEGF [53,54], which is secreted by MSC and binds to VEGFRs on HUVEC (Fig. 5E). Our data indicate that both uPA and uPAR up-regulation in HUVEC and MSC occurs only upon direct but not with indirect co-culture (Fig. 5A, G).

Our data indicate that the uPA-uPAR system promotes ETN formation through several pathways. First, involvement of uPA's catalytic activity is indicated by the finding that ETN formation was reduced by two-thirds in the presence of the uPA enzymatic inhibitor amiloride [55] (Fig. 6B). Enzymatically active uPA initiates a proteolytic cascade involving plasmin generation followed by activation of a subset of MMPs that degrade extracellular matrix proteins and activation/release of matrix-bound pro-angiogenic growth factors, such as basic fibroblast growth factor (bFGF/FGF-2) [19,56], transforming growth factor (TGFβ1) [57], and hepatocyte-derived growth factor (HGF) [58] among others. uPA cleaves/activates the VEGF-A^{189} isoform [18] and HGF [59] directly and indirectly cleaves/activates VEGF-A^{165} and VEGF-A^{189} [60–62] through generation of plasmin. The question, which of these mechanisms is operative in ETN formation, will require additional study.

Second, binding of uPA to its receptor uPAR/CD87 redistributes the enzyme to the leading edge of migrating cells [63–65] and confers partnership with diverse membrane co-receptors [66] that initiate intracellular signaling involved in EC migration [40,67]. In line with this, the uPA-specific monoclonal antibody ATN-292, which recognizes the GFD domain in uPA and prevents its binding to uPAR [39], significantly, albeit incompletely, inhibited ETN formation (Fig. 6A).

Third, our data strongly implicate the association of uPAR and/or its endocytic receptor LRP1 with α_v -containing integrins ($\alpha_v\beta_3$, $\alpha_v\beta_1$ or $\alpha_v\beta_5$) [38,39,68]. To investigate this possibility, we used the anti-uPAR monoclonal Ab ATN-658, which binds to domain 3 of uPAR and prevents its binding to integrins [38] without affecting binding of uPA [38], significantly inhibited ETN formation (Fig. 6A). uPAR binds to $\alpha_v\beta_3$ and $\alpha_v\beta_5$ integrins [25,69,70] and activates cell adhesion and migration [71]. Our data indicate that the neutralizing antibodies to α_v integrin subunit completely blocked ETN formation by HUVEC in co-culture with MSC (Fig. 6A and Supplement Fig. 6), implicating signaling induced by association of α_v integrins with uPAR and extracellular matrix proteins in ETN formation by HUVEC co-cultured with MSC. This suggestion is supported by our data indicating significant up-regulation of β3 integrin subunit in MSC upon co-culture with HUVEC (Fig. 5B). αvβ3 integrin could serve as an adhesion receptor for fibronectin [72]. We observed that MSC-derived fibronectin assembly into the fibrils is critical for the initiation of ETN formation by HUVEC in direct co-culture with MSC (Figs. 3 and 4). Indeed, we observed that extensive branching of ETN structures was happening when fibronectin fibrils were clearly visible by immunofluorescence 48 h after the MSC and HUVEC were brought into direct co-culture (Fig. 3, Table 1), or if MSC were first grown as a monoculture for 48 h to allow fibronectin synthesis and fibril assembly, and HUVEC were then plated on the top of MSC only for 24 h (Fig. 4D-F, and Table 2). This might suggest that uPAR in concert with αvβ3 integrin in MSC promotes fibronectin fibrils assembly, which then facilitates ETN formation by HUVEC directly co-cultured with MSC.

Fourth, catalytically active uPA is rapidly and irreversibly inhibited by its inhibitor PAI-1 [42] and the uPA-PAI-1 complex undergoes internalization via endocytic receptor LRP1 [73]. ETN formation was partially inhibited by the LRP1 antagonist RAP, which blocks internalization of uPAR-bound uPA and uPA-PAI-1 complexes (Fig. 6B,

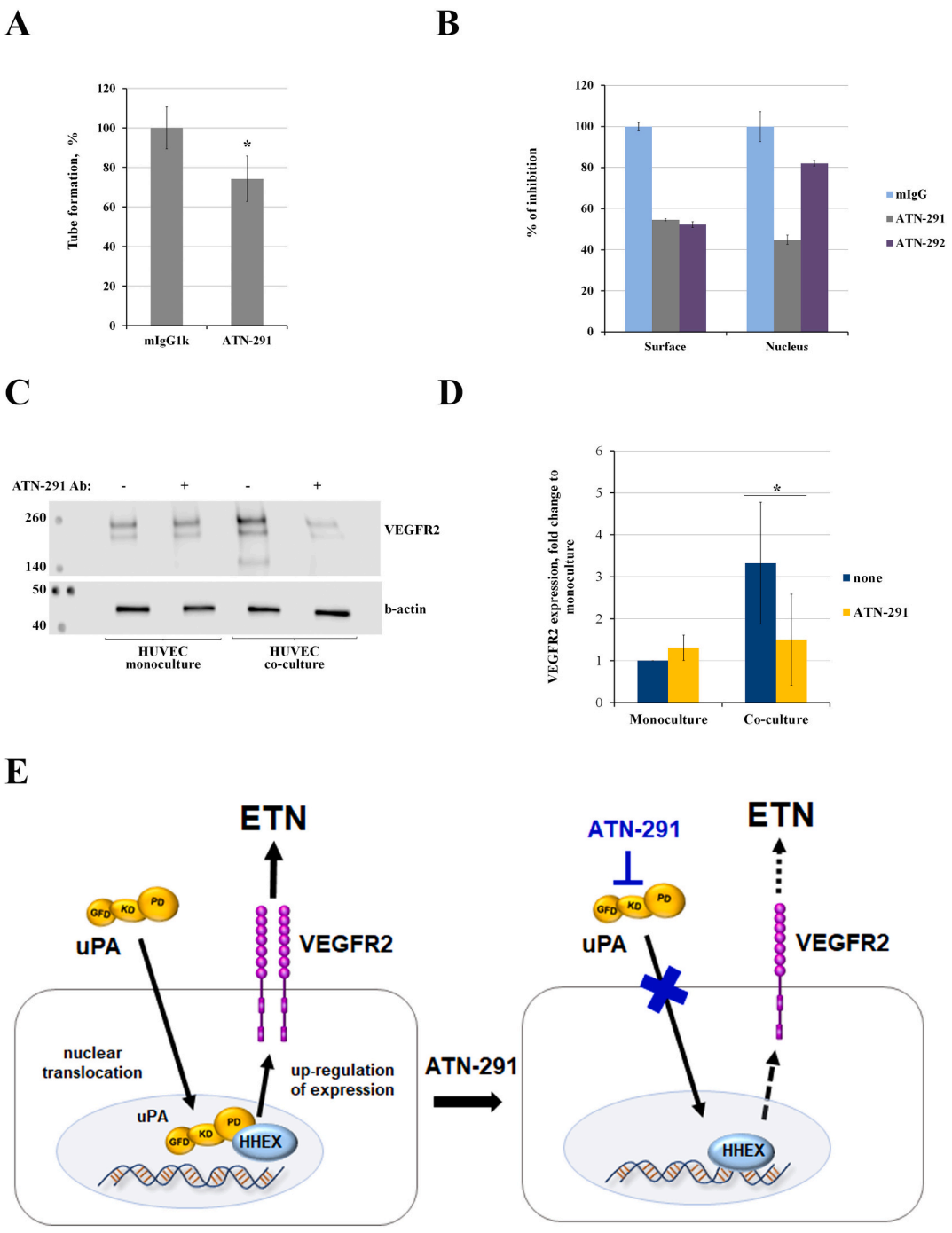

Fig. 7. Blocking the kringle domain of uPA inhibits its nuclear translocation, induction of VEGFR2 and ETN formation by HUVEC in co-culture with MCS. (A) Anti-uPA kringle antibody ATN-291 (180 μg/ml) attenuates ETN formation by HUVEC during co-culture with MSC. Quantification of the total length of the tubular structures formed by HUVEC co-cultured with MSC in the absence or presence of ATN-291 antibody was performed as in Fig. 2B. Y-axis denotes % inhibition. Experiments were performed in triplicate. "*"$P < 0.05$, $N = 3$. (B) Antibody ATN-291 inhibits nuclear translocation of uPA in HUVECs. Confluent HUVEC were incubated with iodinated single-chain uPA (^{125}I-scuPA) for 60 min in presence of ATN-291 antibody, ATN-292 antibody which recognizes GFD in uPA, or mouse IgGk (50 μg/ml each). Subcellular fractions were obtained as described in "Materials and methods". The amount of ^{125}I-scuPA bound to the surface or translocated to the nuclei in the IgGk -treated cells was taken as 100%. Y-axis reflects % inhibition of retention of ^{125}I-scuPA on the surface or in the nuclei of HUVEC. (C) Antibody ATN-291 inhibits up-regulation of VEGFR2 by HUVEC in co-culture with MSC. HUVECs in monoculture or co-cultured with MSC in the absence or presence of ATN-291 antibodies or isotype control IgGk for 48 h. HUVEC and MSC after co-culture were detached, separated using the anti-human ICAM-2-coated magnetic beads to collect HUVEC. HUVEC grown as monoculture were also detached and collected using the anti-human ICAM-2-coated magnetic beads. HUVEC from each experimental condition were lysed and subjected to SDS PAGE and western blotting as described in "Materials and methods" using rabbit anti-VEGFR2 antibodies followed by HRP-conjugated anti-rabbit antibodies, and HRP-conjugated anti-β-actin antibodies as a loading control. Representative WB images are shown. (D) Quantification of the data obtained for Fig. 7C was performed by densitometry analyses of the blots using the Image Studio™ software (LI-COR Biosciences). "*"$P < 0.05$, $n = 3$ experiments. (E) Proposed schematic representation of the signal transduction pathway mediating ETN formation by HUVEC upon VEGFR2 up-regulation in HUVEC by MSC-derived uPA that underwent nuclear translocation in HUVEC during direct HUVEC-MSC co-culture.

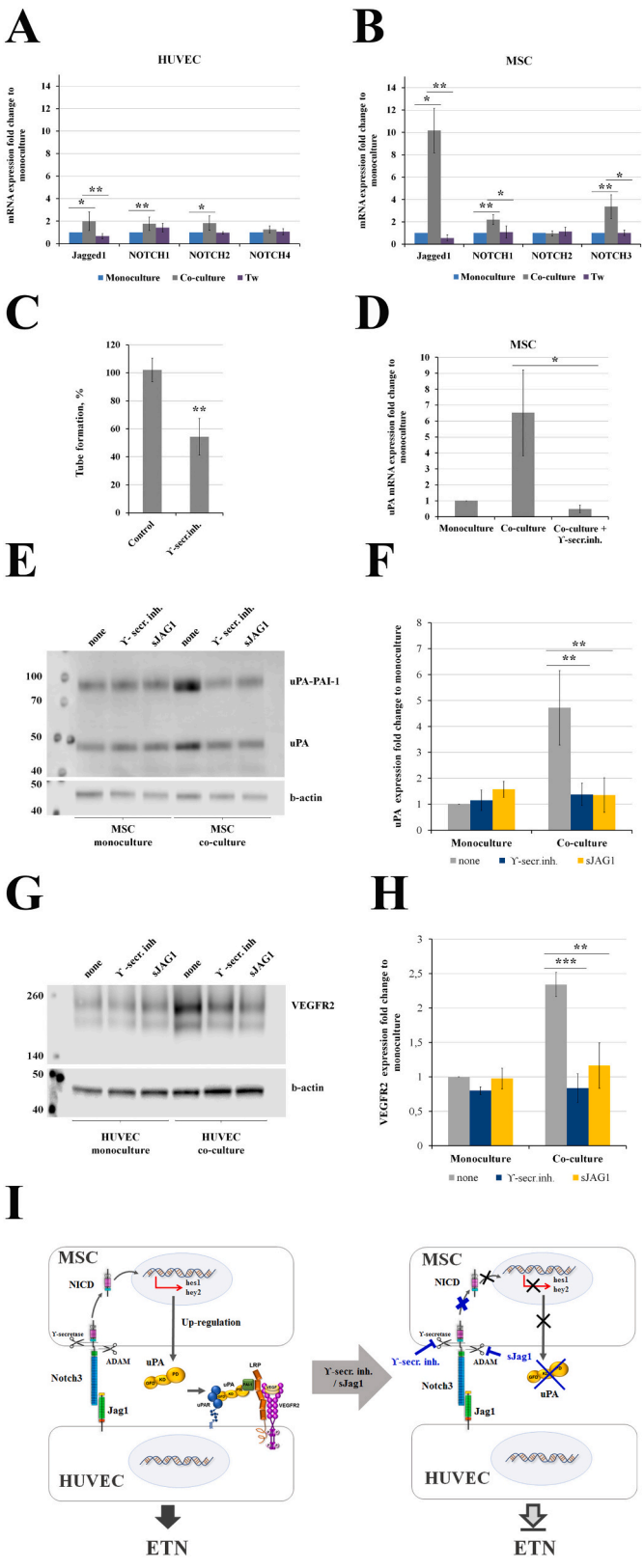

(caption on next page)

Fig. 8. Inhibition of Notch signaling prevents uPA up-regulation and attenuates ETN formation by HUVEC co-cultured with MSC. (A) and (B): Effect of direct or indirect (Transwell) co-culture on mRNA levels of Notch system components in HUVEC and MSC, respectively. Co-culture conditions, cell separation, RNA isolation and mRNA levels were as described in Fig. 5. Quantification of changes in mRNA levels in HUVEC (A) and MSC (B) grown in co-cultures vs corresponding monocultures. Y-axis denotes fold change in mRNA levels of cells in co-culture or Transwell compared to the mRNA levels for the same transcript in either HUVEC or MSC monocultures. "*"P < 0.05, "**": P < 0.005 vs monoculture, n ≥ 3. (C) Effect of inhibitor of γ-secretase Compound E (10 μg/ml) in HUVEC co-cultured with MSC. HUVEC were pre-loaded with cell tracker CMFDA before co-culture with MSC as in Fig. 1. The total length of the tubular structures formed by HUVEC co-cultured with MSC during the ensuing 48 h was quantified using Image J. "**"P < 0.005, $n = 3$. Y-axis denotes % inhibition. (D) Effect of γ-secretase inhibitor Compound E on up-regulation of uPA mRNA in MSC co-cultured with HUVEC. MSC in mono-culture or co-cultured with HUVEC in the absence or presence of Compound E for 24 h. HUVEC were separated from MSC after co-culture using the anti-ICAM-2-coated magnetic beads. MSC from all experimental conditions were pelleted by centrifugation and total RNA was isolated and analyzed as described for Fig. 5A. Y-axis denotes fold change in uPA mRNA levels of MSC in co-culture compared to the mRNA levels in MSC monocultures. "*"P < 0.05, n = 3 experiments. (E) Effect of Compound E and soluble Jagged1-FC (sJAG1) recombinant protein on up-regulation of uPA protein in MSC co-cultured with HUVEC. MSC and HUVEC were grown in mono-cultures or MSC were co-cultured with HUVEC in the absence or presence of Compound E or sJAG1 for 48 h. HUVEC were separated from MSC after co-culture using the anti-ICAM-2-antibody-coated magnetic beads. MSC from all experimental conditions were pelleted by centrifugation, lysed and subjected to SDS PAGE and western blotting. uPA and uPA-PAI-1 complexes in MSC lysates were detected using mouse anti-uPA monoclonal antibodies. Probing of the parallel blot with the HRP-conjugated anti-β-actin antibody was used as the loading control. Representative WB images are shown. (F) Quantification of the data shown in Fig. 8E was performed as described for 7D. "*"P < 0.05, n = 3. (G) HUVEC, collected from co-culture and monoculture using anti-ICAM-2 antibody-coated magnetic beads from the experiment described in panel (E) were lysed and subjected to SDS PAGE and western blotting. VEGFR2 in HUVEC lysates was detected by western blotting as described in Fig. 7C. Representative WB images are shown. (H) Quantification of the data obtained for Fig. 8G was performed as described in 7D. "*"P < 0.05, n = 3. (I) Proposed schematic representation of uPA expression and regulation in MSC upon direct co-culture with HUVEC via NOTCH signal transduction pathway.

Supplement Fig. 7). LRP1 acts as a signaling receptor for uPA–PAI-1-induced G_s activation, resulting in the upregulation of cAMP level, activation of PKA and eNOS [74] and increased endothelial permeability [35,75], which frequently accompanies angiogenesis [76].

LRP1 also forms a multireceptor complex with VEGF receptor 2 (VEGFR2), β1-integrin, and uPAR on the membrane of ECs that mediates endocytosis of the entire complex upon binding of VEGF, leading to phosphorylation of VEGFR2 and activation of ERK [77]. VEGFR-2, activated primarily by VEGF-A, plays a key role in the transduction of angiogenic signals and controls EC morphology, chemotaxis, and proliferation [1,78]. VEGFR2 association with $\alpha_v\beta_3$ leads to the activation of VEGFR2 [79–81]. We observed that HUVEC VEGFR2 mRNA is upregulated in direct co-culture with MSC compared to HUVEC grown as a monoculture (Fig. 5A). Moreover, the VEGFR2 antagonist DMH4

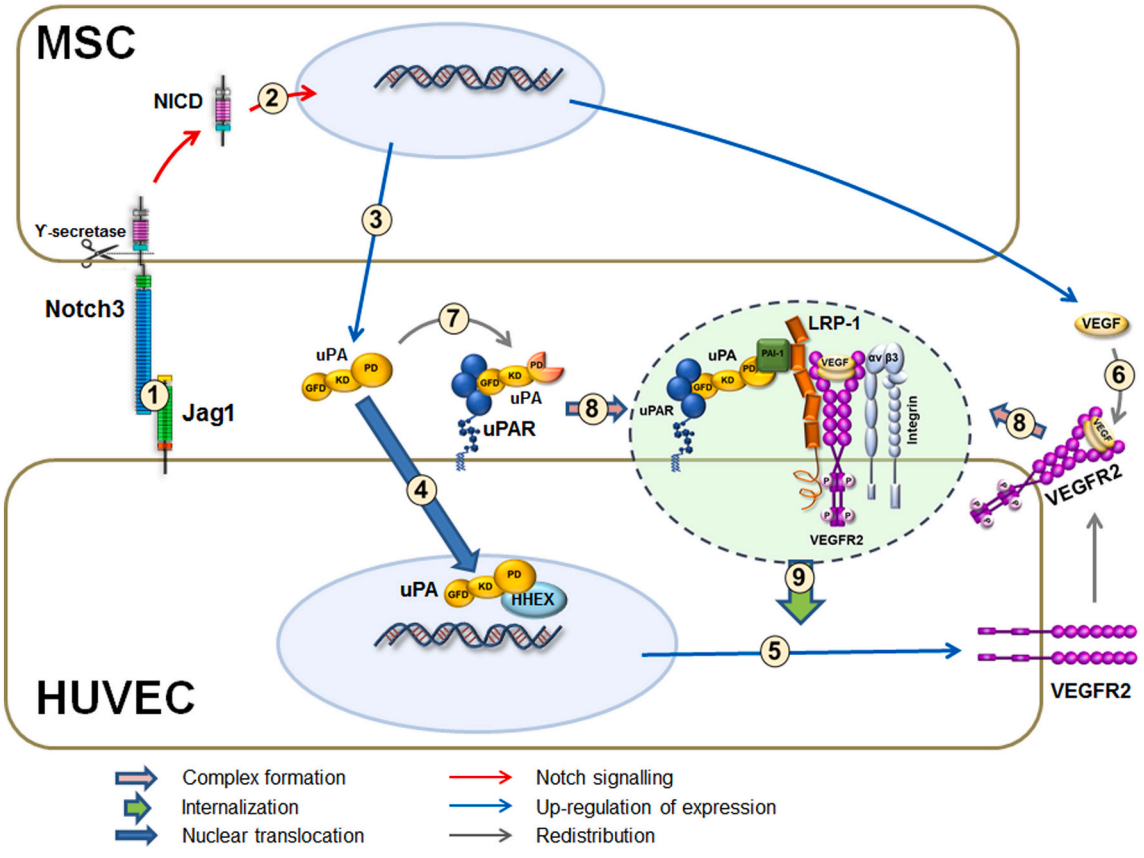

Fig. 9. ETN formation by HUVEC in direct co-culture with MSC requires uPA/uPAR, VEGF/VEGFR2, $\alpha_v\beta_3$ integrins, Notch-activated signaling and LRP1 driven endocytosis. "1" – The interaction of the Notch 3 receptor on MSC with Jagged 1 ligand on HUVEC is followed by γ-secretase-mediated Notch receptor cleavage and generation of NICD. "2" nuclear translocation of NICD leads to target genes transcription activation. "3" Notch-induced upregulation of uPA expression in MSC. "4" Secreted scuPA translocates to HUVEC nuclei and binds HHEX transcription repressor. "5" scuPA de-represses VEGFR2 promoter and thereby up-regulates VEGFR2. "6" VEGF secreted by MSC binds VEGFR2 on HUVEC surface. "7" secreted scuPA binds uPAR, is converted to catalytically active tcuPA, which is followed by inhibition by PAI-1. "8" uPAR-bound tcuPA-PAI-1 complexes interact with LRP1, which is engaged with VEGFR2 and $\alpha_v\beta_3$ integrin. "9" A multicomponent complex undergoes endocytosis driven by LRP1 followed by ETN formation.

inhibited ETN formation in co-culture (Fig. 6C, Supplement Fig. 7), implicating VEGFR2 in the process. Whether DMH4 disrupts the association of VEGFR2 with $\alpha_v\beta_3$ and/or uPAR and/or LRP1 requires further investigation.

The mechanisms controlling VEGF and VEGFR-2 expression are only partly understood [78]. Our data indicate that direct co-culture of HUVECs with MSC for 24 h results in up-regulation of VEGF mRNA in HUVEC (Fig. 5A). However, MSC express and secrete significantly higher levels of VEGF than do HUVEC in monoculture (Fig. 5E). MSC might be the primary source of VEGF, which in turn activates HUVEC. There was a significant drop in VEGF protein in the conditioned media of co-cultured HUVEC-MSC compared to MSC in monoculture (Fig. 5E). We hypothesize that VEGF secreted by MSC in co-culture binds to VEGFRs on the HUVEC surface, which induces over-expression of uPAR on HUVEC (Fig. 5A) as reported by others [75,82]. This accelerates internalization and subsequent signal transduction via LRP1/VEGFR2/α_v integrins/uPA-PAI-1-uPAR complex [77,83] (see Fig. 9 for summary).

Fifth, we have shown that scuPA translocates to the nuclei of ECs in a kringle-dependent manner and up-regulates expression of VEGFR2 by blocking the transcriptional repressor HHEX/PRH [12]. Our data indicate that this mechanism is also operative during ETN formation. The anti-uPA kringle ATN-291 antibody [39], which attenuates ETN formation by HUVEC in presence of MSC (Fig. 7A), inhibits nuclear translocation of uPA in HUVECs (Fig. 7B) and blocks up-regulation of VEGFR2 in HUVEC upon co-culture with MSC co-culture (Fig. 7C).

Sixth, our data indicate that Notch signaling is activated in both cell pools upon co-culture of HUVEC with MSC (Fig. 8A and B), supporting data reported previously by other groups [84,85]. Our data indicate that inhibition of γ-secretase significantly reduced ETN formation in HUVECs-MSCs co-culture (Fig. 8C). uPA over-expression in MSC co-cultured with HUVEC could be mediated by JAG1-Notch receptor signaling as has been reported for breast cancer cell lines [45]. In support of this hypothesis, overexpression of uPA in MSC co-cultured with HUVEC (Fig. 5B, D) was abrogated by a γ-secretase inhibitor Compound E and by receptor competition with recombinant soluble Jagged1 ligand (sJAG1) [86] (Fig. 8D, E and F) concomitant with inhibition of VEGFR2 expression in HUVEC co-cultured with MSC (Fig. 8G and H). The latter data further support the role of uPA-mediated transcriptional activity in paracrine regulation of VEGFR2 expression in endothelial cells upon communications with mesenchymal cells via Notch system components. Together, the studies reported here strongly implicate the uPA/uPAR system in ETN formation and thereby in endothelial capillary formation in vivo. They indicate that each of the identified functions of the ligand/receptor pair is involved in the angiogenic process: catalytic activity, binding to uPAR, crosstalk with VEGF/VEGFR2, α_v integrins and Notch signaling pathways, nuclear translocation and gene transcription (Fig. 9). Although uPA catalytic activity and uPAR levels are implicated in pathogenic processes such as cancer, inhibitors of either protein have not been successful in clinical trials [87,88]. Our data help to explain this finding and suggest that it may be necessary to simultaneously target multiple uPA-mediated pathways to control aberrant angiogenesis with minimal impact on healthy vasculature.

Supplementary data to this article can be found online at https://doi.org/10.1016/j.bbamcr.2021.119157.

Declarations

Not applicable.

Funding

This work was supported by the Russian Foundation for Basic Research 19-015-00511 (IB), Russian Science Foundation 17-15-01368П (KD), USAMRMC # TS150032, and the LAM Foundation # LAM0139P07-19 (VS).

CRediT authorship contribution statement

IB, VS, KD, EZ, YP contributed to the conception and experimental design. IB, VS, EZ, KD, NK performed cell isolation and co-culture experiments. NK, OP, EZ performed flow cytometry. DD performed cell sorting. PAT-K performed co-culture video on Nikon Eclipse Ti microscope. APM provided guidance with antibodies to uPAR. VS, KD performed experiments involving translocation of uPA to cell nuclei, immunoblotting analysis. IB and NK performed ELISA. IB and EZ performed RNA isolation, reverse transcription and real-time quantitative PCR. IB, VS, and KD analyzed the data and wrote the manuscript. VS, YP and DBC revised the manuscript. All authors read and approved the final manuscript.

Declaration of competing interest

The authors declare no competing interests.

Acknowledgements

We thank George Sharonov (Lomonosov Moscow State University) and Mikhail Menshikov (National Medical Research Center for Cardiology) for assistance with flow cytometry experiments and Jillian Evans (University of Pennsylvania) for critical reading of the Manuscript.

References

[1] R.H. Adams, K. Alitalo, Molecular regulation of angiogenesis and lymphangiogenesis, Nat. Rev. Mol. Cell Biol. (2007), https://doi.org/10.1038/nrm2183.
[2] M. Potente, H. Gerhardt, P. Carmeliet, Basic and therapeutic aspects of angiogenesis, Cell (2011), https://doi.org/10.1016/j.cell.2011.08.039.
[3] P. Carmeliet, Angiogenesis in life, disease and medicine, Nature (2005), https://doi.org/10.1038/nature04478.
[4] A.S. Chung, N. Ferrara, Developmental and pathological angiogenesis, Annu. Rev. Cell Dev. Biol. (2011), https://doi.org/10.1146/annurev-cellbio-092910-154002.
[5] R.E. Gilbert, The endothelium in diabetic nephropathy, Curr. Atheroscler. Rep. 16 (2014) 410, https://doi.org/10.1007/s11883-014-0410-8.
[6] J. Sottile, Regulation of angiogenesis by extracellular matrix, Biochim. Biophys. Acta - Rev. Cancer (2004), https://doi.org/10.1016/j.bbcan.2003.07.002.
[7] V. Ranta, T. Mikkola, O. Ylikorkala, L. Viinikka, A. Orpana, Reduced viability of human vascular endothelial cells cultured on Matrigel, J. Cell. Physiol. 176 (1998) 92–98, https://doi.org/10.1002/(SICI)1097-4652(199807)176:1<92::AID-JCP11>3.0.CO;2-Q.
[8] S. Merfeld-Clauss, N. Gollahalli, K.L. March, D.O. Traktuev, Adipose tissue progenitor cells directly interact with endothelial cells to induce vascular network formation, Tissue Eng. A 16 (2010) 2953–2966, https://doi.org/10.1089/ten.tea.2009.0635.
[9] L. Evensen, D.R. Micklem, A. Blois, S.V. Berge, N. Aarsaether, A. Littlewood-Evans, J. Wood, J.B. Lorens, Mural cell associated VEGF is required for organotypic vessel formation, PLoS One (2009), https://doi.org/10.1371/journal.pone.0005798.
[10] N. Montuori, P. Ragno, Role of uPA/uPAR in the modulation of angiogenesis, Chem. Immunol. Allergy 99 (2014) 105–122, https://doi.org/10.1159/000353310.
[11] F. Blasi, N. Sidenius, The urokinase receptor: focused cell surface proteolysis, cell adhesion and signaling, FEBS Lett. 584 (2010) 1923–1930, https://doi.org/10.1016/j.febslet.2009.12.039.
[12] V. Stepanova, P.S. Jayaraman, S.V. Zaitsev, T. Lebedeva, K. Bdeir, R. Kershaw, K. R. Holman, Y.V. Parfyonova, E.V. Semina, I.B. Beloglazova, V.A. Tkachuk, D. B. Cines, Urokinase-type plasminogen activator (upa) promotes angiogenesis by attenuating proline-rich homeodomain protein (prh) transcription factor activity and de-repressing vascular endothelial growth factor (vegf) receptor expression, J. Biol. Chem. 291 (2016) 15029–15045, https://doi.org/10.1074/jbc.M115.678490.
[13] S. Kasai, H. Arimura, M. Nishida, T. Suyama, Primary structure of single-chain pro-urokinase, J. Biol. Chem. 260 (22) (1985) 12382–12389.
[14] C.M. Ghajar, S. Kachgal, E. Kniazeva, H. Mori, S.V. Costes, S.C. George, A. J. Putnam, Mesenchymal cells stimulate capillary morphogenesis via distinct proteolytic mechanisms, Exp. Cell Res. 316 (2010) 813–825, https://doi.org/10.1016/j.yexcr.2010.01.013.
[15] S. Kasai, H. Arimura, M. Nishida, T. Suyama, Proteolytic cleavage of single-chain pro-urokinase induces conformational change which follows activation of the zymogen and reduction of its high affinity for fibrin, J. Biol. Chem. 260 (22) (1985) 12377–12381.
[16] P. Carmeliet, L. Moons, D. Collen, Mouse models of angiogenesis, arterial stenosis, atherosclerosis and hemostasis, Cardiovasc. Res. (1998), https://doi.org/10.1016/S0008-6363(98)00108-4.

[17] A.P. Mazar, J. Henkin, R.H. Goldfarb, The urokinase plasminogen activator system in cancer: implications for tumor angiogenesis and metastasis, Angiogenesis (1999), https://doi.org/10.1023/A:1009095825561.
[18] J. Plouët, F. Moro, S. Bertagnolli, N. Coldeboeuf, H. Mazarguil, S. Clamens, F. Bayard, Extracellular cleavage of the vascular endothelial growth factor 189-amino acid form by urokinase is required for its mitogenic effect, J. Biol. Chem. (1997), https://doi.org/10.1074/jbc.272.20.13390.
[19] O. Saksela, D.B. Rifkin, Release of basic fibroblast growth factor-heparan sulfate complexes from endothelial cells by plasminogen activator-mediated proteolytic activity, J. Cell Biol. (1990), https://doi.org/10.1083/jcb.110.3.767.
[20] V.W.M. Van Hinsbergh, M.A. Engelse, P.H.A. Quax, Pericellular proteases in angiogenesis and vasculogenesis, Arterioscler. Thromb. Vasc. Biol. (2006), https://doi.org/10.1161/01.ATV.0000209518.58252.17.
[21] Y. Wei, D.A. Waltz, N. Rao, R.J. Drummond, S. Rosenberg, H.A. Chapman, Identification of the urokinase receptor as an adhesion receptor for vitronectin, J. Biol. Chem. 269 (1994) 32380–32388.
[22] N. Sidenius, F. Blasi, Domain 1 of the urokinase receptor (uPAR) is required for uPAR-mediated cell binding to vitronectin, FEBS Lett. (2000), https://doi.org/10.1016/S0014-5793(00)01282-5.
[23] W. Xue, I. Mizukami, R.F. Todd, H.R. Petty, Urokinase-type plasminogen activator receptors associate with β1 and β3 integrins of fibrosarcoma cells: dependence on extracellular matrix components, Cancer Res. 57 (9) (1997) 1682–1689.
[24] P. Franco, I. Vocca, M.V. Carriero, D. Alfano, L. Cito, I. Longanesi-Cattani, P. Grieco, L. Ossowski, M.P. Stoppelli, Activation of urokinase receptor by a novel interaction between the connecting peptide region of urokinase and αvβ5 integrin, J. Cell Sci. (2006), https://doi.org/10.1242/jcs.03067.
[25] Y. Wei, M. Lukashev, D.I. Simon, S.C. Bodary, S. Rosenberg, M.V. Doyle, H. A. Chapman, Regulation of integrin function by the urokinase receptor, Science (80-.) (1996), https://doi.org/10.1126/science.273.5281.1551.
[26] Y. Wei, J.A. Eble, Z. Wang, J.A. Kreidberg, H.A. Chapman, Urokinase receptors promote β1 integrin function through interactions with integrin α3β1, Mol. Biol. Cell (2001), https://doi.org/10.1091/mbc.12.10.2975.
[27] J.T. Parsons, K.H. Martin, J.K. Slack, J.M. Taylor, S.A. Weed, Focal adhesion kinase: a regulator of focal adhesion dynamics and cell movement, Oncogene. 19 (2000) 5606–5613, https://doi.org/10.1038/sj.onc.1203877.
[28] E.D. Sprengers, C. Kluft, Plasminogen activator inhibitors, Blood (1987), https://doi.org/10.1182/blood.v69.2.381.381.
[29] T.W. Stief, K.P. Radtke, N. Heimburger, Inhibition of urokinase by protein C-inhibitor (PCI). Evidence for identity of PCI and plasminogen activator inhibitor 3, Biol. Chem. Hoppe Seyler 368 (1987) 1427–1433, https://doi.org/10.1515/bchm3.1987.368.2.1427.
[30] A. Nykjaer, M. Conese, E.I. Christensen, D. Olson, O. Cremona, J. Gliemann, F. Blasi, Recycling of the urokinase receptor upon internalization of the uPA:serpin complexes, EMBO J. (1997), https://doi.org/10.1093/emboj/16.10.2610.
[31] M.V. Cubellis, T.C. Wun, F. Blasi, Receptor-mediated internalization and degradation of urokinase is caused by its specific inhibitor PAI-1, EMBO J. (1990), https://doi.org/10.1002/j.1460-2075.1990.tb08213.x.
[32] P.H. Jensen, E.I. Christensen, P. Ebbesen, J. Gliemann, P.A. Andreasen, Lysosomal degradation of receptor-bound urokinase-type plasminogen activator is enhanced by its inhibitors in human trophoblastic choriocarcinoma cells, Mol. Biol. Cell (1990), https://doi.org/10.1091/mbc.1.13.1043.
[33] L. Goretzki, B.M. Mueller, Receptor-mediated endocytosis of urokinase-type plasminogen activator is regulated by cAMP-dependent protein kinase, J. Cell Sci. 110 (Pt 12) (1997) 1395–1402.
[34] Z. Ma, K.S. Thomas, D.J. Webb, R. Moravec, A.M. Salicioni, W.M. Mars, S. L. Gonias, Regulation of Rac1 activation by the low density lipoprotein receptor-related protein, J. Cell Biol. (2002), https://doi.org/10.1083/jcb.200207070.
[35] A.M. Makarova, T.V. Lebedeva, T. Nassar, A.A.R. Higazi, J. Xue, M.E. Carinato, K. Bdeir, D.B. Cines, V. Stepanova, Urokinase-type plasminogen activator (uPA) induces pulmonary microvascular endothelial permeability through low density lipoprotein receptor-related protein (LRP)-dependent activation of endothelial nitric-oxide synthase, J. Biol. Chem. 286 (2011) 23044–23053, https://doi.org/10.1074/jbc.M110.210195.
[36] V. Stepanova, T. Lebedeva, A. Kuo, S. Yarovoi, S. Tkachuk, S. Zaitsev, K. Bdeir, I. Dumler, M.S. Marks, Y. Parfyonova, V.A. Tkachuk, A.A.-R. Higazi, D.B. Cines, Nuclear translocation of urokinase-type plasminogen activator, Blood. 112 (2008) 100–110, https://doi.org/10.1182/blood-2007-07-104455.
[37] B. Baudin, A. Bruneel, N. Bosselut, M. Vaubourdolle, A protocol for isolation and culture of human umbilical vein endothelial cells, Nat. Protoc. (2007), https://doi.org/10.1038/nprot.2007.54.
[38] X. Xu, Y. Cai, Y. Wei, F. Donate, J. Juarez, G. Parry, L. Chen, E.J. Meehan, R. W. Ahn, A. Ugolkov, O. Dubrovskyi, T.V. O'Halloran, M. Huang, A.P. Mazar, Identification of a new epitope in uPAR as a target for the cancer therapeutic monoclonal antibody ATN-658, a structural homolog of the uPAR binding integrin CD11b (αM), PLoS One 9 (2014), https://doi.org/10.1371/journal.pone.0085349.
[39] T.V. O'Halloran, R. Ahn, P. Hankins, E. Swindell, A.P. Mazar, The many spaces of uPAR: delivery of theranostic agents and nanobins to multiple tumor compartments through a single target, Theranostics. 3 (2013) 496–506, https://doi.org/10.7150/thno.4953.
[40] I.B. Beloglazova, E.S. Zubkova, D.V. Stambol'skii, O.S. Plekhanova, M. Y. Men'shikov, Z.A. Akopyan, R.S. Bibilashvili, E.V. Parfenova, V.A. Tkachuk, Proteolytically inactive recombinant forms of urokinase suppress migration of endothelial cells, Bull. Exp. Biol. Med. 156 (2014) 756–759, https://doi.org/10.1007/s10517-014-2442-z.
[41] M.V. Cubellis, P. Andreasen, P. Ragno, M. Mayer, K. Danø, F. Blasi, Accessibility of receptor-bound urokinase to type-1 plasminogen activator inhibitor, Proc. Natl. Acad. Sci. U. S. A. 86 (1989) 4828–4832, https://doi.org/10.1073/pnas.86.13.4828.
[42] S. Thorsen, M. Philips, J. Selmer, I. Lecander, B. Astedt, Kinetics of inhibition of tissue-type and urokinase-type plasminogen activator by plasminogen-activator inhibitor type 1 and type 2, Eur. J. Biochem. 175 (1988) 33–39, https://doi.org/10.1111/j.1432-1033.1988.tb14162.x.
[43] G. Bu, S. Rennke, Receptor-associated protein is a folding chaperone for low density lipoprotein receptor-related protein, J. Biol. Chem. (1996), https://doi.org/10.1074/jbc.271.36.22218.
[44] R.L. Kendall, R.Z. Rutledge, X. Mao, A.J. Tebben, R.W. Hungate, K.A. Thomas, Vascular endothelial growth factor receptor KDR tyrosine kinase activity is increased by autophosphorylation of two activation loop tyrosine residues, J. Biol. Chem. (1999), https://doi.org/10.1074/jbc.274.10.6453.
[45] M. Shimizu, B. Cohen, P. Goldvasser, M. Shimizu, B. Cohen, P. Goldvasser, H. Berman, C. Virtanen, Plasminogen Activator uPA is a Direct Transcriptional Target of the JAG1-Notch Receptor Signaling Pathway in Breast Cancer Plasminogen Activator uPA Is a Direct Transcriptional Target of the JAG1-Notch Receptor Signaling Pathway in Breast Cancer, 2011, https://doi.org/10.1158/0008-5472.CAN-10-2523.
[46] I.W. Tattersall, J. Du, Z. Cong, B.S. Cho, A.M. Klein, C.L. Dieck, R.A. Chaudhri, H. Cuervo, J.H. Herts, J. Kitajewski, In vitro modeling of endothelial interaction with macrophages and pericytes demonstrates Notch signaling function in the vascular microenvironment, Angiogenesis vol. 19 (2016) 201–215, https://doi.org/10.1007/s10456-016-9501-1.
[47] T. Kangsamaksin, A. Murtomaki, N.M. Kofler, H. Cuervo, R.A. Chaudhri, I. W. Tattersall, P.E. Rosenstiel, C.J. Shawber, J. Kitajewski, NOTCH decoys that selectively block DLL/NOTCH or JAG/NOTCH disrupt angiogenesis by unique mechanisms to inhibit tumor growth, Cancer Discov. 5 (2015) 182–197, https://doi.org/10.1158/2159-8290.CD-14-0650.
[48] T. Yang, D. Arslanova, Y. Gu, C. Augelli-szafran, W. Xia, Quantification of gamma-secretase modulation differentiates inhibitor compound selectivity between two substrates Notch and amyloid precursor protein 13 (2008) 1–13, https://doi.org/10.1186/1756-6606-1-15.
[49] C.R. Dass, P.F.M. Choong, Cancer angiogenesis: targeting the heel of Achilles, J. Drug Target. 16 (2008) 449–454, https://doi.org/10.1080/10611860802088523.
[50] J. Glade-Bender, J.J. Kandel, D.J. Yamashiro, VEGF blocking therapy in the treatment of cancer, Expert. Opin. Biol. Ther. 3 (2003) 263–276, https://doi.org/10.1517/14712598.3.2.263.
[51] C.M. Andreoli, J.W. Miller, Anti-vascular endothelial growth factor therapy for ocular neovascular disease, Curr. Opin. Ophthalmol. 18 (2007) 502–508, https://doi.org/10.1097/ICU.0b013e3282f0ca54.
[52] H.A. Elshabrawy, Z. Chen, M.V. Volin, S. Ravella, S. Virupannavar, S. Shahrara, The pathogenic role of angiogenesis in rheumatoid arthritis, Angiogenesis. 18 (2015) 433–448, https://doi.org/10.1007/s10456-015-9477-2.
[53] M.E. Kroon, P. Koolwijk, M.A. Vermeer, B. Van Der Vecht, V.W.M. Van Hinsbergh, Vascular endothelial growth factor enhances the expression of urokinase receptor in human endothelial cells via protein kinase C activation, Thromb. Haemost. 85 (2001) 296–302, https://doi.org/10.1055/s-0037-1615683.
[54] S.J. Mandriota, G. Seghezzi, J.D. Vassalli, N. Ferrara, S. Wasi, R. Mazzieri, P. Mignatti, M.S. Pepper, Vascular endothelial growth factor increases urokinase receptor expression in vascular endothelial cells, J. Biol. Chem. (1995), https://doi.org/10.1074/jbc.270.17.9709.
[55] J.D. Vassalli, D. Belin, Amiloride selectively inhibits the urokinase-type plasminogen activator, FEBS Lett. 214 (1987) 187–191, https://doi.org/10.1016/0014-5793(87)80039-X.
[56] P. Koolwijk, M.G.M. Van Erck, W.J.A. De Vree, M.A. Vermeer, H.A. Weich, R. Hanemaaijer, V.W.M. Van Hinsbergh, Cooperative effect of TNF, bFGF, and VEGF on the formation of tubular structures of human microvascular endothelial cells in a fibrin matrix, in: Role of Urokinase Activity 132, 1996.
[57] J. Taipale, K. Koli, J. Keski-Oja, Release of transforming growth factor-β1 from the pericellular matrix of cultured fibroblasts and fibrosarcoma cells by plasmin and thrombin, J. Biol. Chem. 267 (35) (1992) 25378–25384.
[58] H. Matsuoka, T.H. Sisson, T. Nishiuma, R.H. Simon, Plasminogen-mediated activation and release of hepatocyte growth factor from extracellular matrix, Am. J. Respir. Cell Mol. Biol. 35 (2006) 705–713, https://doi.org/10.1165/rcmb.2006-0006OC.
[59] L. Naldini, L. Tamagnone, E. Vigna, M. Sachs, G. Hartmann, W. Birchmeier, Y. Daikuhara, H. Tsubouchi, F. Blasi, P.M. Comoglio, Extracellular proteolytic cleavage by urokinase is required for activation of hepatocyte growth factor/scatter factor, EMBO J. 11 (1992) 4825–4833.
[60] N. Ferrara, Binding to the extracellular matrix and proteolytic processing: two key mechanisms regulating vascular endothelial growth factor action, Mol. Biol. Cell (2010), https://doi.org/10.1091/mbc.E09-07-0590.
[61] J.E. Park, G.A. Keller, N. Ferrara, The vascular endothelial growth factor (VEGF) isoforms: differential deposition into the subepithelial extracellular matrix and bioactivity of extracellular matrix-bound VEGF, Mol. Biol. Cell (1993), https://doi.org/10.1091/mbc.4.12.1317.
[62] K.A. Houck, D.W. Leung, A.M. Rowland, J. Winer, N. Ferrara, Dual regulation of vascular endothelial growth factor bioavailability by genetic and proteolytic mechanisms, J. Biol. Chem. 267 (1992) 26031–26037.
[63] H. McNeill, P.J. Jensen, A high-affinity receptor for urokinase plasminogen activator on human keratinocytes: characterization and potential modulation during migration, Mol. Biol. Cell (1990), https://doi.org/10.1091/mbc.1.11.843.
[64] A. Estreicher, J. Mühlhauser, J.L. Carpentier, L. Orci, J.D. Vassalli, The receptor for urokinase type plasminogen activator polarizes expression of the protease to the

leading edge of migrating monocytes and promotes degradation of enzyme inhibitor complexes, J. Cell Biol. 111 (1990) 783–792, https://doi.org/10.1083/jcb.111.2.783.
[65] G.W. Prager, J.M. Breuss, S. Steurer, D. Olcaydu, J. Mihaly, P.M. Brunner, H. Stockinger, B.R. Binder, Vascular endothelial growth factor receptor-2-induced initial endothelial cell migration depends on the presence of the urokinase receptor, Circ. Res. 94 (2004) 1562–1570, https://doi.org/10.1161/01.RES.0000131498.36194.6b.
[66] H.W. Smith, C.J. Marshall, Regulation of cell signalling by uPAR, Nat. Rev. Mol. Cell Biol. 11 (2010) 23–36, https://doi.org/10.1038/nrm2821.
[67] K.S. Kim, Y. Hong, Y.A. Joe, Y. Lee, J. Shin, H. Park, I. Lee, S. Lee, D. Kang, S. Chang, S. Il Chung, Anti-angiogenic Activity of the Recombinant Kringle Domain of Urokinase and Its Specific Entry Into Endothelial Cells 278, 2003, pp. 11449–11456, https://doi.org/10.1074/jbc.M212358200.
[68] S.A. Rabbani, B. Ateeq, A. Arakelian, M.L. Valentino, D.E. Shaw, L.M. Dauffenbach, C.A. Kerfoot, A.P. Mazar, An anti-urokinase plasminogen activator receptor antibody (ATN-658) blocks prostate cancer invasion, migration, growth, and experimental skeletal metastasis in vitro and in vivo, Neoplasia 12 (2010) 778–788, https://doi.org/10.1593/neo.10296.
[69] T. Tarui, A.P. Mazar, D.B. Cines, Y. Takada, Urokinase-type plasminogen activator receptor (CD87) is a ligand for integrins and mediates cell-cell interaction, J. Biol. Chem. 276 (2001) 3983–3990, https://doi.org/10.1074/jbc.M008220200.
[70] M.V. Carriero, S. Del Vecchio, M. Capozzoli, P. Franco, L. Fontana, A. Zannetti, G. Botti, G. D'Aiuto, M. Salvatore, M.P. Stoppelli, Urokinase receptor interacts with α(v)β5 vitronectin receptor, promoting urokinase-dependent cell migration in breast cancer, Cancer Res. 59 (20) (1999) 5307–5314.
[71] P. Ragno, The urokinase receptor: a ligand or a receptor? Story of a sociable molecule, Cell. Mol. Life Sci. 63 (2006) 1028–1037, https://doi.org/10.1007/s00018-005-5428-1.
[72] I.F. Charo, L. Nannizzi, J.W. Smith, D.A. Cheresh, The vitronectin receptor alpha v beta 3 binds fibronectin and acts in concert with alpha 5 beta 1 in promoting cellular attachment and spreading on fibronectin, J. Cell Biol. 111 (1990) 2795–2800, https://doi.org/10.1083/jcb.111.6.2795.
[73] J. Herz, D.E. Clouthier, R.E. Hammer, LDL receptor-related protein internalizes and degrades uPA-PAI-1 complexes and is essential for embryo implantation, Cell. 71 (1992) 411–421, https://doi.org/10.1016/0092-8674(92)90511-a.
[74] L. Goretzki, B.M. Mueller, Low-density-lipoprotein-receptor-related protein (LRP) interacts with a GTP-binding protein, Biochem. J. 336 (Pt 2) (1998) 381–386, https://doi.org/10.1042/bj3360381.
[75] M.A. Behzadian, L.J. Windsor, N. Ghaly, G. Liou, N.-T. Tsai, R.B. Caldwell, VEGF-induced paracellular permeability in cultured endothelial cells involves urokinase and its receptor, FASEB J. Off. Publ. Fed. Am. Soc. Exp. Biol. 17 (2003) 752–754, https://doi.org/10.1096/fj.02-0484fje.
[76] J.A. Nagy, L. Benjamin, H. Zeng, A.M. Dvorak, H.F. Dvorak, Vascular permeability, vascular hyperpermeability and angiogenesis, Angiogenesis. 11 (2008) 109–119, https://doi.org/10.1007/s10456-008-9099-z.
[77] S. Herkenne, C. Paques, O. Nivelles, M. Lion, K. Bajou, T. Pollenus, M. Fontaine, P. Carmeliet, J.A. Martial, N.-Q.-N. Nguyen, I. Struman, The interaction of uPAR with VEGFR2 promotes VEGF-induced angiogenesis, Sci. Signal. 8 (2015), ra117, https://doi.org/10.1126/scisignal.aaa2403.
[78] M. Shibuya, L. Claesson-Welsh, Signal transduction by VEGF receptors in regulation of angiogenesis and lymphangiogenesis, Exp. Cell Res. 312 (2006) 549–560, https://doi.org/10.1016/j.yexcr.2005.11.012.
[79] P.R. Somanath, N.L. Malinin, T.V. Byzova, Cooperation between integrin alphavbeta3 and VEGFR2 in angiogenesis, Angiogenesis. 12 (2009) 177–185, https://doi.org/10.1007/s10456-009-9141-9.
[80] R. Soldi, S. Mitola, M. Strasly, P. Defilippi, G. Tarone, F. Bussolino, Role of α(v)β3 integrin in the activation of vascular endothelial growth factor receptor-2, EMBO J. (1999), https://doi.org/10.1093/emboj/18.4.882.
[81] G.H. Mahabeleshwar, J. Chen, W. Feng, P.R. Somanath, O.V. Razorenova, T. V. Byzova, Integrin affinity modulation in angiogenesis, Cell Cycle 7 (2008) 335–347, https://doi.org/10.4161/cc.7.3.5234.
[82] Y. Feng, V.J. Venema, R.C. Venema, N. Tsai, M.A. Behzadian, R.B. Caldwell, VEGF-induced permeability increase is mediated by caveolae, Invest. Ophthalmol. Vis. Sci. 40 (1999) 157–167.
[83] G.A. LaRusch, A. Merkulova, F. Mahdi, Z. Shariat-Madar, R.G. Sitrin, D.B. Cines, A. H. Schmaier, Domain 2 of uPAR regulates single-chain urokinase-mediated angiogenesis through β1-integrin and VEGFR2, Am. J. Physiol. Heart Circ. Physiol. 305 (2013), https://doi.org/10.1152/ajpheart.00110.2013.
[84] T. Liang, L. Zhu, W. Gao, M. Gong, J. Ren, H. Yao, K. Wang, Coculture of endothelial progenitor cells and mesenchymal stem cells enhanced their proliferation and angiogenesis through PDGF and Notch signaling 7 (2017) 1722–1736, https://doi.org/10.1002/2211-5463.12317.
[85] Y. Tachida, N. Izumi, T. Sakurai, H. Kobayashi, Mutual Interaction Between Endothelial Cells and Mural Cells Enhances BMP9 Signaling in Endothelial Cells, 2017, pp. 370–380, https://doi.org/10.1242/bio.020503.
[86] K.N. Lovendahl, S.C. Blacklow, W.R. Gordon, The molecular mechanism of notch activation, in: T. Borggrefe, B.D. Giaimo (Eds.), Mol. Mech. Notch Signal, Springer International Publishing, Cham, 2018, pp. 47–58, https://doi.org/10.1007/978-3-319-89512-3_3.
[87] N. Mahmood, C. Mihalcioiu, S.A. Rabbani, Multifaceted role of the urokinase-type plasminogen activator (uPA) and its receptor (uPAR): diagnostic, prognostic, and therapeutic applications, Front. Oncol. 8 (2018), https://doi.org/10.3389/fonc.2018.00024.
[88] M. Vincenza Carriero, M. Patrizia Stoppelli, The urokinase-type plasminogen activator and the generation of inhibitors of urokinase activity and signaling, Curr. Pharm. Des. 17 (2011) 1944–1961, https://doi.org/10.2174/138161211796718143.